RFP-3020
August 10, 1981

RFP-3020
August 10, 1981

PROCESSING AND STRUCTURE OF HIGH-ENERGY-RATE-FORGED 21-6-9 AND 304L FORGINGS

M. C. Mataya

M. J. Carr

R. W. Krenzer

G. Krauss

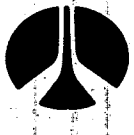

Rockwell International

Energy Systems Group
Rocky Flats Plant
P.O. Box 464
Golden, Colorado 80401

U. S. DEPARTMENT OF ENERGY
CONTRACT DE-AC04-76DP03533

DISCLAIMER

Printed
August 10, 1981

RFP-3020
UC-25 MATERIALS
DOE/TIC-4500 (Rev. 69)

PROCESSING AND STRUCTURE OF HIGH-ENERGY-RATE-FORGED 21-6-9 AND 304L FORGINGS

M. C. Mataya

M. J. Carr

R. W. Krenzer

G. Krauss

G. A. Riordan, Editor

L. M. Morales, Compositor

ROCKWELL INTERNATIONAL
ENERGY SYSTEMS GROUP
ROCKY FLATS PLANT
P.O. BOX 464
GOLDEN, COLORADO 80401

Prepared under Contract DE-AC04-76DP03533
for the
Albuquerque Operations Office
U.S. Department of Energy

CONTENTS

ABSTRACT

Two 304L and three Nitronic 40 (21-6-9) high energy rate processed forgings were studied to determine interrelationships that exist between forging history, mechanical properties, microstructure, macrostructure, and substructure. A striking observation is the wide variation in properties and structure between different forgings and also between different locations within an individual forging. Variations were related to either finishing temperature of the last forming stage or to the forming sequence. For example, lower finishing temperatures resulted in higher dislocation densities; and therefore higher strengths. Higher finishing temperatures promoted dynamic recrystallization, lower dislocation densities, and lower strengths. With respect to forming sequence, locations in the forging which are formed first undergo a number of additional thermal cycles while the rest of the part is being formed. These areas are usually recrystallized and have lower dislocation densities, and therefore lower strengths relative to locations formed later in the sequence.

The observations made in this report highlight the important relationship between substructure, mechanical properties, and forging history and have put into perspective the metallurgical considerations that play a role in developing final properties.

PROCESSING AND STRUCTURE OF HIGH ENERGY RATE FORGED 21-6-9 AND 304L FORGINGS

M. C. Mataya, M. J. Carr, R. W. Krenzer, and G. Krauss

INTRODUCTION

High energy rate forging (HERF) is used extensively in the weapons community to produce complex, high strength, austenitic stainless steel forgings. Characteristically, the forgings are required to meet specified mechanical and microstructural properties. Most often, annealed strengths are not suitable for the design application. Austenitic stainless steels such as 304L and Nitronic 40 (21-6-9) cannot be significantly strengthened by precipitation hardening after forging. Therefore, high strengths must be imparted during fabrication. HERF processing has been effective in producing high strengths by the introduction of a dense dislocation substructure. Sanderson, et al.,[1] showed that substructure in 21-6-9 HERF processed forgings consisted of cells composed of loosely tangled dislocations, and this effect on metallurgical properties is discussed in detail.

Generally, during working at conventional strain rates, dislocation cells form below (cold work) and subgrains above (hot work) 0.4 T_m to 0.5 T_m where T_m is the melting point in degrees Kelvin.[2,3] However, the high strain rates of HERF (800 S^{-1}) extend the hot work transition temperature to at least 0.6 T_m.[1] Cold working results in a rapid buildup of strength with deformation without softening due to recovery or recrystallization. Hot working is deformation carried out at temperatures where recrystallization occurs almost simultaneously with deformation. As a result, a hot worked structure will not be work hardened as much as a cold worked structure given the same amount of deformation. Since the high strain rates of HERF tend to extend the cold working temperature to higher temperatures, strengths in HERF processed parts would be expected to be higher than those in Press Forged (PF) parts formed at the same temperatures. Recent results indicate that this occurs in JBK-75.[4] Also, Sanderson, et al.,[1] showed that PF can impart high strengths by the introduction of dislocation cells during cold working. However, it appears that the duplexed substructure of cells and subgrains observed in HERF forgings result in significantly increased ductility at equivalent strength.

Although HERF processing can produce desirable mechanical properties and structures, a number of unexpected and unexplained problems have arisen in process development and production. For example, processing of 304L usually includes a short time anneal of the final forging. This anneal serves as a stress relief. Generally, high strengths imparted in forging are maintained. On occasion, however, a particular forging lot will be "dead soft" and fail to meet specified strengths.[5] Since furnace time is a specified constant, some change in metallurgical structure imparted to the forgings during processing causes this anomolous behavior. This report addresses itself to characterizing such changes in structure.

Hardness traverses on forgings frequently show significant gradients in mechanical properties from one location to another.[6-8] Furthermore, the hardness of a particular location in a forging may vary significantly in different forging lots.[1,9] In general, hardness correlates with strength,[7,9] and therefore the hardness variations indicate nonuniformity in strength within a single forging.

Typical forgings have lug stems protruding from a hemispherical body. Characteristically, there is a significant transition in strength and hardness from stem to body. Generally, soft stems are desired which can accommodate additional cold work during assembly operations without cracking. Although these mechanical property differences exist, light microscopy often shows similar microstructures. In fact, certain anomolies have been recorded. For example, coarse grained areas may be stronger than fine grained areas. Elongated grains,

apparently cold worked, may be weaker than areas which are equiaxed and appear to be fully recrystallized. These anomolies are explained by the nature of the substructure within the grains. The substructure is too fine to be revealed by light microscopy and is revealed only by transmission electron microscopy (TEM).

Another problem has been a locally heterogeneous distribution of work which often leads to folds in the grain flow, feathered areas, or adiabatic shear bands. Such forging defects cause concern because of expected discontinuities in mechanical properties associated with the effects. In addition, transverse grain flow in the wall of the forging may result. This condition must be avoided in critical applications. The service behavior of forgings with these defects has not been well characterized. However, the catastrophic effect of transverse grain flow coupled with a brittle second phase, i.e., sigma, on tensile properties has been well documented.[10]

Low forging temperatures are often used to achieve high strengths. As a result, the microstructures of 21-6-9 forgings often show carbide precipitation. There has been concern that the carbides will degrade corrosion resistance and environmental compatibility. In addition, recent work on JBK-75[11] shows that second phase precipitates may degrade forgeability, promote flow localization and, in the end, result in adiabatic shear bands. Therefore, when considering forging defects, final forging at low temperatures and high strain rates may cause problems. Continued effort must be made to better define the critical variables which affect forgeability.

Frequently, processes go out of control with respect to metallurgical quality. Properties are a function of structure imparted during forging. In turn, structure is a function of the interdependent variables of strain rate (the speed at which the metal flows) processing temperature, time at temperature, strain (amount of deformation given to the metal), and applied stress at which the metal flows. Stress can be a function of die design, lubrication, and tool wear. A delicate balance exists between these process variables. Without proper control, significant changes in metallurgical structure and properties may occur.

The control of HERF processing is important because of critical design requirements for the forgings. However, the problems and anomolies discussed above show that more needs to be learned about the interrelationships of forging history, structure, and properties. Thus, the complexity of processing control remains an important practical concern. In the end, improved control will result in increased forging quality and a decreased rejection rate in production.

Because of the importance of the deformation process on the resulting mechanical properties of steel, it is instructive to consider the effect of processing variables in some detail. Within the regime of strain rates used in HERF processing and forging geometries discussed in this work, very limited information exists in the metallurgical literature. Work hardening steel forgings by HERF processing is not extensively used outside the weapons complex. To provide a background for the analysis discussed in this report, the following section, Literature Review, is included. The section deals with the effect of processing variables on microstructure, substructure, and resulting mechanical properties.

Literature Review

Workability, structure (including macrostructure, microstructure, and substructure), and mechanical properties of a metal depend on the stress level attained during processing, the strain imparted, and the strain rate of forming, the temperature at which the metal is deformed, and the time at temperature. The lack of information on the interdependencies of these five processing variables and how workability, structure, and properties are affected make the design of processing criteria qualitative at best. Process development occurs, of necessity, by trial and error and is, in part, redundant for new parts which are similar.

In apparently simple operations such as extrusion and rolling, strain rate varies in a complex way with reduction and location.[12] Closed die forging is an even more complex forming process. Parameters such as chamber shape, lubrication, die staging, temperature, forging pressure, strain rate, and

handling time can all be highly variable and, in turn, may lead to significant variations in the final product. The following is a discussion of the interdependencies of stress, strain, strain rate, time, and temperature during mechanical processing and their effect on structure and mechanical properties. It should become obvious that knowledge of substructure, as it is developed in processing and as it affects properties, is necessary for establishing processing design criteria and/or the troubleshooting of processing problems.

1. Cold Working and Recovery

Upon deforming a metal, dislocations are generated. At first, dislocations are few and well separated but with increasing deformation the dislocation density increases and tangles form. The tangles link up, forming interconnected walls with relatively dislocation free areas between the walls.[2] This structure is commonly referred to as a dislocation cell structure and is produced by cold work below 0.5 T_m. Figure 1

FIGURE 1. Comparison of Dislocation Substructure Formation During Cold Working, Recovery, and Hot Working or Creep

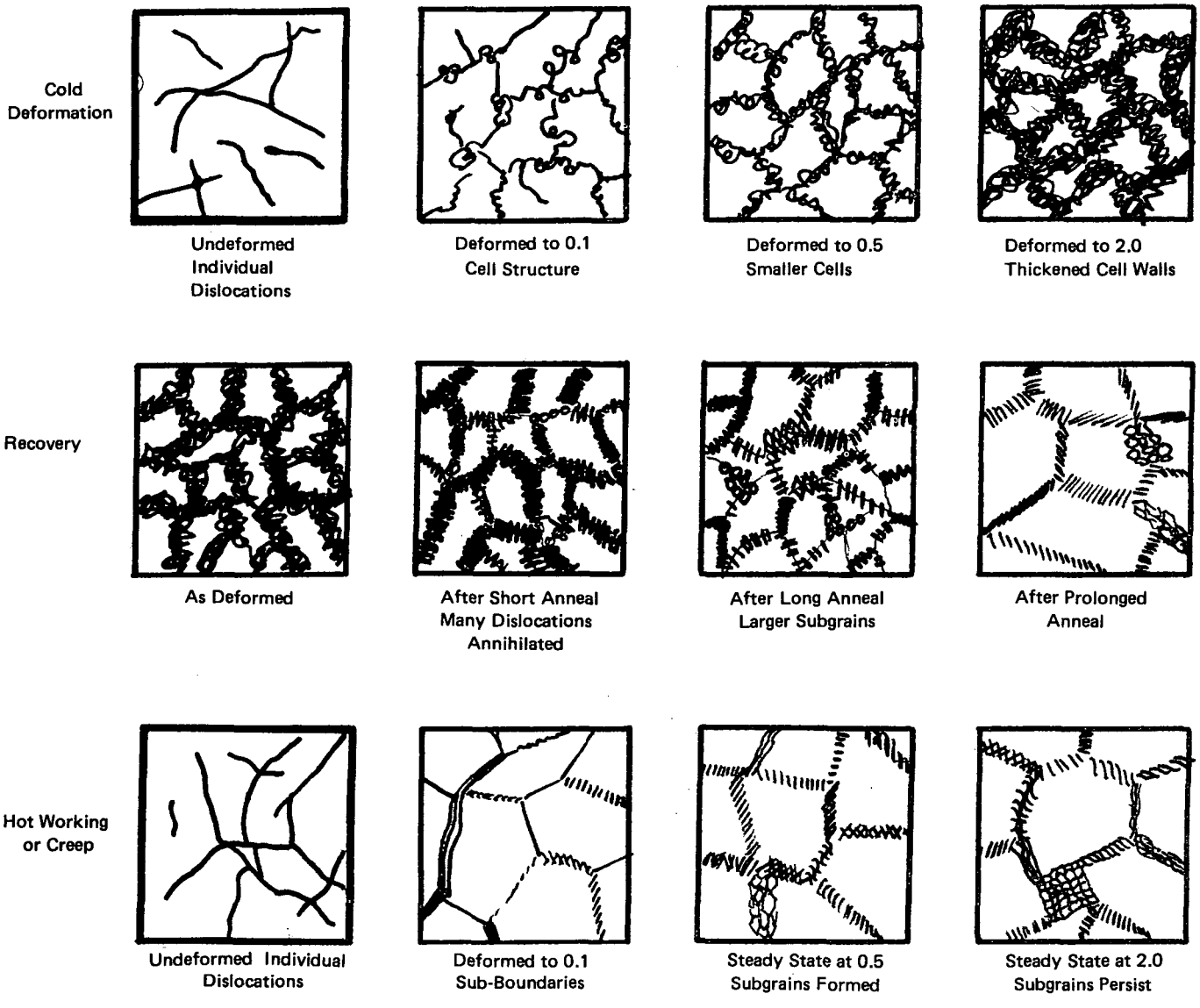

shows a schematic representation of the development of the cell structure with increasing strain. Mechanical strength is inversely related to cell size (diameter).[3] As the deformation temperature is raised, the characteristic cell size for a particular strain level increases, dislocation density drops, and strength is reduced. The dislocations become arranged in more geometrically regular networks and a transition from cold to hot working occurs.

During heating after cold working, the dislocations in the cells rearrange themselves to form subgrains, a process sometimes referred to as polygonization, Figure 1. During this stage of heating sometimes called recovery, dislocations, move, aided by thermal energy in the crystal lattice and internal stress fields of the dislocation arrays. As a result, the dislocations are annihilated or rearranged into low energy, subgrain boundaries. Subgrains can also increase in size during annealing, further reducing strength.

2. Hot Working

High temperature deformation testing has shown that metals will initially undergo strain hardening. During this flow, stress is a complex function of strain. However, after initial strain hardening a steady state region ensures where stress is independent of strain.[12] In materials such as copper and copper alloys, nickel and nickel alloys, and austenitic steels, steady state is preceded by work softening and at low strain rates by oscillations in the stress strain curve.[13, 14] Both phenomenon have been related to dynamic recrystallization (recrystallization which occurs during deformation). Figure 2a shows this behavior schematically. The oscillations occur because of successive periods of strain hardening and subsequent dynamic recrystallization. Eventually, the oscillations dampen out as the recrystallization events become out of phase at different locations in the sample. The structural variations which occur within a simple test specimen during deformation indicate that much greater variations could be expected in different areas of complex-shaped forgings.

On the other hand, aluminum and aluminum alloys, commercial purity α-iron, and ferritic iron alloys strain harden to steady state without softening and recrystallization, as shown in Figure 2b. The dislocation density increases during hardening, gradually forms subgrains, and stabilizes in the steady state regime where dislocations are annihilated at the same rate that they are generated.[13] The subgrains may remain equiaxed within the elongating grains. This behavior is accomplished by continual decomposition and reformation of the subgrain boundaries, a process sometimes referred to as repolygonization.[15] Dislocations interacting to reduce the amount of strain hardening during metal working (exclusive of dynamic recrystallization processes) is often referred to as dynamic

FIGURE 2. Stress-Strain Behavior for Materials Exhibiting (a) Dynamic Recrystallization and (b) Dynamic Recovery During Hot Deformation

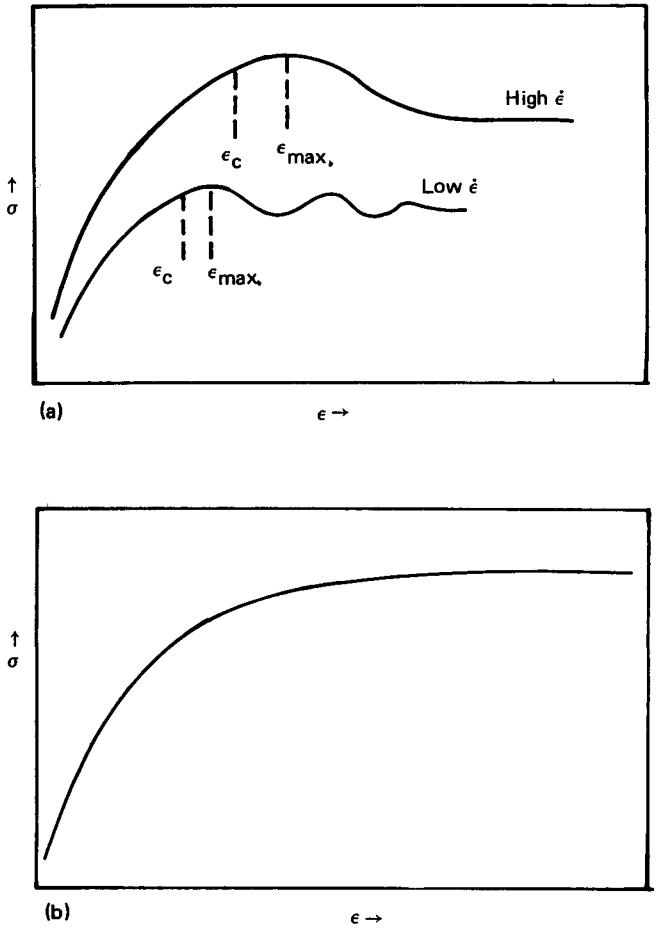

recovery. Repolygonization and dislocation annihilation are two mechanisms of dynamic recovery.

If deformation temperature is raised or the strain rate lowered, the probability of dislocation interaction, a thermally activated event, is increased per unit strain or time.[12] Dislocation density drops and subgrain size increases, and results in reduced strength. This type of dynamic recovery is favored in metals with high stacking fault energies (SFE), i.e., aluminum. The dislocations are highly mobile as a result of easy cross slip and can rearrange themselves into subgrain boundaries rapidly enough to keep up with deformation. This has been demonstrated in such processes as rolling and extrusion.[2] In metals with low SFE, i.e., 304L, dislocation mobility is reduced. During deformation then the dislocation substructure cannot maintain a steady state configuration. Dislocation density increases to a critical value at which time dynamic recrystallization occurs by the coalescence of several adjacent subgrains. As a result, dislocation density and strength drop rapidly. It has been found that high strain rates inhibit coalescence and, therefore, dynamic recrystallization.[14]

In the steady state regime of hot working, strain no longer remains a functional variable. Process control is thus somewhat simplified. In this regime the flow stress, σ, has been expressed as a product of strain rate and an exponential term containing temperature. The product is referred to as the Zener-Holloman parameter, and is written as follows:[16]

$$f(\sigma) = \dot{\epsilon} \exp\left(\frac{\Delta H}{RT}\right) \qquad (1)$$

where $\dot{\epsilon}$ is strain rate, ΔH is the activation energy for the process (i.e., recovery, recrystallization), R is a constant, and T is temperature (°K). This Arrhenius-type exponential equation implies that the rate-controlling mechanism is thermally activated. In other words, thermal energy in the crystal structure will aid the process. At higher temperatures, more thermal energy is available and therefore the process will be more likely to occur, and at a higher rate.

Equation 1 shows that if the strain rate, $\dot{\epsilon}$, for hot working is increased (i.e., HERF instead of Press), assuming a constant forging temperature, the required flow stress to deform the metal will be greater. On the other hand, a lower flow stress can be achieved if the processing temperature is raised. Dynamically recrystallized grain size has been shown to be inversely related to flow stress.[14] Thus, for higher strain rates and lower temperatures forged strengths should be higher.

Dynamic recrystallization occurs during forming. As a result, any newly recrystallized structure will receive additional work before forming is completed. Therefore, dynamically recrystallized substructures will have a higher dislocation density and higher mechanical strength compared to fully annealed or statically recrystallized structures. A hot worked structure, whether it be dynamically recrystallized or not, may also recrystallize after forming is complete. This is generally referred to as static recrystallization and will be discussed later.

Forming at different strain rates can result in significantly different structures and mechanical properties. For example, at higher strain rates, more strain will have to be imparted for initiation of dynamic recrystallization (ignoring adiabatic heating).[14] This means that for the same forming sequence, a high strain rate may result in strain hardening and a slower rate in recrystallization. Figure 3 shows the various types of behavior.

FIGURE 3. Effect of Strain Rate on Stress-Strain Curves of Pure Ni Deformed at 934 °C

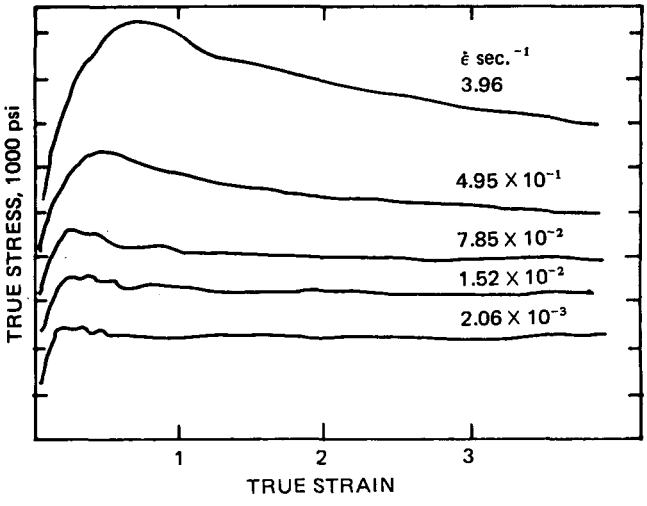

Mechanical property differences produced by strain hardening and recrystallization are significant and, therefore, strain rate is an important process control variable.

Any complex forging will receive different amounts of strain depending upon its location. Since structure and properties are dependent on strain, as shown in Figure 3, homogeneity is nearly precluded. However, a large degree of homogeneity may be achieved by appropriate die and forge temperature sequencing. Generally, however, variations in furnace and forging temperature will occur, and inhomogeneity from part to part can be expected. Automated forging operations would ensure greater reproducibility from part to part.

After deformation is completed, static recrystallization may occur. The rate of recrystallization increases with increasing post deformation temperature, higher residual strains, higher strain rates, and lower stacking fault energy (SFE).[2] With either a higher strain rate, lower forming temperature, or lower SFE, the dislocation subgrains in which the strain is stored will be smaller with extremely tangled, high energy walls.[2] Coalescence of these dislocations around strain free areas will occur more rapidly, resulting in increased recrystallization rates. Static recrystallization results in a dramatic and complete loss of strain hardening accrued during hot working. Microstructure and properties are essentially those of a fully annealed material. Static recrystallization can be prevented or minimized by water quenching after each forming step.

Some metals, such as copper and austenitic carbon steel which have poor ability for dynamic recovery, will statically recrystallize within seconds after hot working.[2] With repetitive recrystallization between rolling stages it has been possible to produce very fine grained steel sheet with high strength and toughness.[2] If the austenitic stainless steels also undergo rapid static recrystallization, then the time between HERF and water quenching will be an important control variable to minimize property scatter in the forgings.

Second Phase Effects

So far only single-phase alloys have been considered. Second phase precipitates can greatly reduce dislocation mobility, thus tend to slow recovery and recrystallization processes. Austenitic stainless steels may be forged with or without second phase carbides. HERF processing of 304L and 21-6-9 is characteristically sequenced over a falling temperature range. The initial forging stages are at high temperatures in the single phase (1800 - 2200 °F) region, whereas latter stages are at temperatures within the carbide precipitation range (1100 - 1600 °F). Carbides can form on heating for forging, or at the forging temperature, or on cooling. In addition to retarding recovery and recrystallization, the carbides can strengthen the metal during forming and thereby reduce workability.[17]

Effect of Substructure on Properties

The effect of size and type of substructure on yield strength can be expressed by a generalized Petch type equation:[3]

$$\sigma_y = \sigma_o + K_s d_s^{-m} \qquad (2)$$

where σ_y is the substructure dependent yield strength, K_s is a constant related to sub-boundary strength, and d_s is the substructure size or diameter. The substructure may consist of cells, subgrains, or grains. The coefficient m appears to be dependent on substructure type; $m = 1/2$ for grains and subgrains and $m = 1$ for cells.[3] For a mixture of cells and subgrains, $1/2 < m < 1$.[3] However, values of $m = 1.5$ have been reported for aluminum.[15] Owing to their high m, cells should be more effective strengtheners over a certain range in size. Young and Sherby[18] showed that below $d_s = 0.4\ \mu m$ cell boundary strengthening surpasses subgrain and grain boundary strengthening as shown in Figure 4. The detailed mechanisms for strengthening are not understood but appear to be related to the character of the substructure boundary and structure size which, in turn, appear to affect the behavior of dislocation sources.[3]

In addition to boundary strengthening, a random dislocation density also has a strengthening effect.

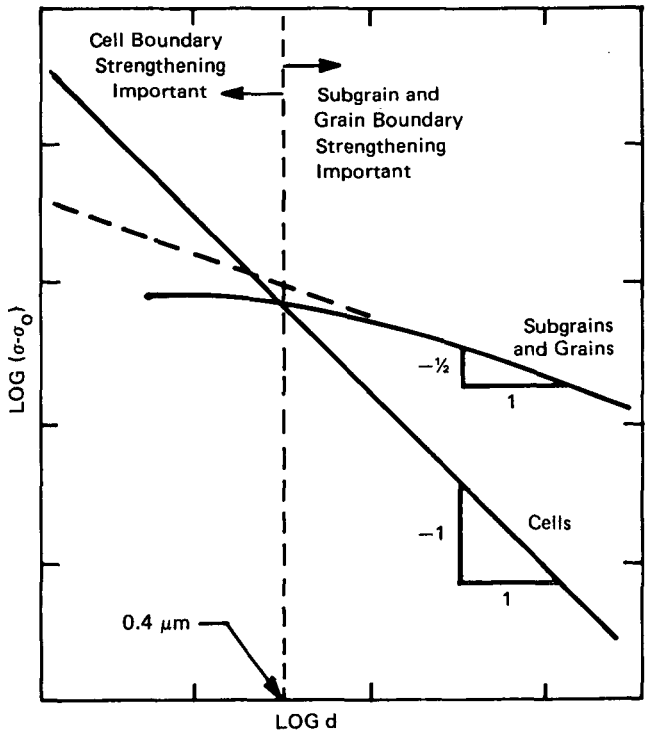

FIGURE 4. Schematic Representation of Strengthening Caused By Grains and Subgrains

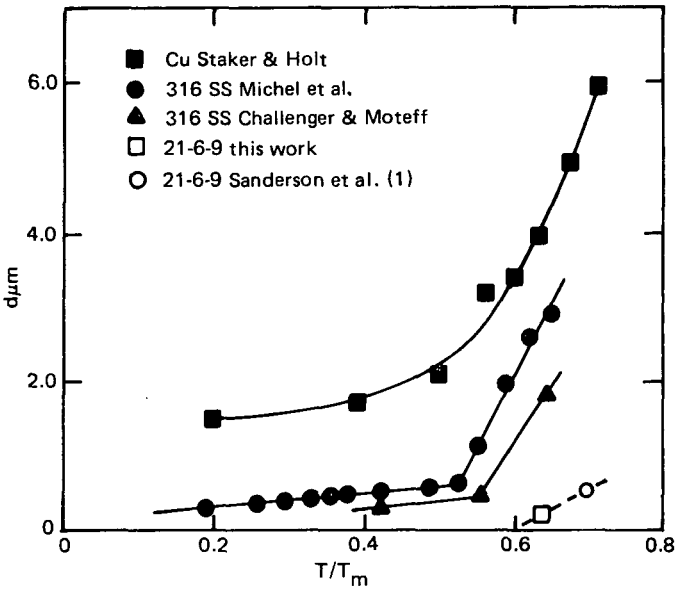

FIGURE 5. Mean Dislocation Cell or Subgrain Diameter Versus T/T_m for 316 Stainless Steel and Copper

Strengthening is known to be a function of the dislocation density, γ, where yield strength is proportional to the square root of the density[3] according to the equation:

$$\sigma_y = \sigma_o + K\sqrt{\gamma} \qquad (3)$$

where σ_o includes all other strengthening except that caused by dislocations, and K is a constant. Understanding the effect of processing on substructure generation can yield improved mechanical properties. For example, a recovered steel (0.13 wt % C) rolled 82% has significantly improved uniform elongation at the same strength level when compared to the cold rolled 62% condition;[19] perhaps this is due to subtle variations in substructures. Nitronic 40 (21-6-9) which has been heavily hot worked and then warm rolled in the stress relieving range has significantly improved ductilities at equivalent yield strengths when compared to hot worked PF or HERF forgings, or hot worked and then cold worked plate.[20] Improved compression yield strengths have been achieved in mild and high strength low alloy steels by prestraining in tension at warm working temperatures (approximately 900 °F).[21] Similarly, tension-compression yield strength differences as-well-as orientation dependence of yield strength have been reduced in high strength 21-6-9 hemishells by forming at 482 °C (900 °F) instead of at room temperature.[22] Increased deformation rates have resulted in increased strength and reduced ductility in 304L[23] and JBK-75.[10]

It has been shown that dynamically recrystallized copper[14] increases in strength with a corresponding change in Z, Zener-Holloman parameter, (with increasing strain rate or a lower deformation temperature). Michel, et al.,[24] showed for 316 stainless steel that cells form below 0.5 T_m. The cell size increased slowly with temperatures between 0.18 T_m and 0.5 T_m. Therefore, a slight drop in strength can be expected as deformation temperature rises in this range. Above 0.5 T_m, subgrains form instead of cells. As shown in Figure 5, the subgrain size is very sensitive to temperature, increasing rapidly as deformation temperature is increased. A relatively rapid loss in strength can be expected above 0.5 T_m.

Sanderson, et al.,[1] showed that cells are formed as high as 0.6 T_m in 21-6-9. Evidently the high strain rate of HERF extends the cold working range upward. Again, strain rate affects substructure and resulting strength. In addition, the same studies showed that HERF forgings had improved ductility at equivalent yield strengths when compared to PF forgings. The improvement could be attributed to the mixed, cell and subgrain, substructure of the HERF parts compared to the relatively cold worked substructure of the PF parts which consisted only of cells.

Owing to the complexity of processing variables, improvements in control of forming processes will result only after increased sophistication in analysis becomes a habit. The analysis will have to include relating the forging history to structure (macrostructure, microstructure, and substructure) and, in turn, to mechanical properties. In any one complex forging, local variations in temperature, strain, strain rate, and stress will exist. Because structure and properties are dependent not only on the combination of instantaneous values of these variables, but also on their history during processing, one can appreciate the difficulty in controlling a forming sequence to produce a specific result.

If static recrystallization occurred between each forging stage, processing control would be simplified. Final metallurgical quality would be imparted in only the last stage. However, if static recrystallization does not occur because of alloy characteristics (i.e., high SFE) or by design (water quenching after each stage), then substructure is retained from one stage to the next and the end result is a function of the cumulative processing history. Although the latter situation is complex and difficult to deal with, it may, in fact, produce the most desirable combinations of structure and properties. HERF processing of austenitic stainless steel weapon components falls within the more complex description.

Purpose

The purpose of this investigation was to better characterize HERF processed stainless steel forgings with respect to forging history, macrostructure, microstructure, substructure, and mechanical properties. Five forgings of different geometry were investigated. Two alloys were selected, 304L and 21-6-9, to evaluate both low and high strength austenitic stainless steels. Both alloys are currently enjoying wide usage. Both bodies and stems have been examined to characterize the range of metallurgical differences that may exist in any one forging. This characterization coupled with past[1, 11] and current[4, 10] efforts should be helpful in generating improved forging design criteria and process control.

Experimental Procedure

Five different forging shapes were selected for study and assigned the working designation of A, R, B, L, and S used throughout this report. Table 1 provides complete heat and forging control identification for the austenitic stainless steels used for the five forgings. As shown in Table 1, the 304L was Vacuum-Arc-Remelted (VAR), and the 21-6-9 was Electro-Slag-Remelted (ESR). Table 2 lists the chemical compositions of the heats of steel used for the forgings. Figure 6 shows the shapes of the forgings. A variety of shapes were selected to produce a large range of deformation histories. Experience[5] with similar forgings has shown that substantial differences in microstructure and properties are often present between the bodies and stems of some of the forgings. These differences are sometimes desirable for processing subsequent to forging, and are characterized in detail throughout Sections A through E of Results and Discussion section of this report.

Table 3 presents the processing histories of the five forgings. Homologous temperatures of the fractions of the melting temperature (T/T_m) at which the various forging stages were performed are also listed. The melting temperatures were taken at 1355 °C, the solidus for WR specified 21-6-9 stainless steel[1] and 1400 °C, the solidus for 304L stainless steel.[25] The calculation of T/T_m was performed after converting both the processing temperature and the solidus temperature to absolute temperature by adding 273 to the degrees centigrade.

TABLE 1. Heat and Forging Control Identification

Forging Identification*	Heat	Mill	Melt	Material Control No.	Stock Type	Forging Lot No.
A (304L)	50050-3	Car. Tech.	VAR	104009	2 1/2 in. Dia. Bar	1362
R (304L)	17485-1	Car. Tech.	VAR	105809	4 in. Dia. Bar	3205
B (21-6-9)	7298-4	Simonds	ESR	104462	1 3/4 in. Plate	1398A-B
L (21-6-9)	7653-2	Simonds	ESR	105287	2 in. Dia. Bar	2505
S (21-6-9)	91023-1	Car. Tech.	ESR	104696	2 in. Dia. Bar	1712

*Internal Rocky Flats Designation

TABLE 2. Chemical Compositions of Austenitic Stainless Steels Used in Forgings

Forging Identification*	C	N	Cr	Ni	Mn	Mo	P	Si	S	Co	Al (ppm)	O (ppm)
A (304L)	0.015	0.042	18.5	10.4	1.5	< 0.25	< 0.04	0.6	0.006	< 0.20	–	–
R (304L)	0.016	0.038	18.6	10.8	1.8	0.10	0.02	0.65	0.004	0.07	–	–
B (21-6-9)	0.024	0.278	19.7	7.26	8.59	–	< 0.02	0.24	0.008	–	50	10
L (21-6-9)	0.029	0.30	19.6	7.13	9.19	–	0.019	0.47	< 0.003	–	20	20
S (21-6-9)	0.028	0.30	20.0	6.85	9.15	–	< 0.02	0.38	0.002		200	< 10

*Internal Rocky Flats Designation

Table 4 lists the mechanical properties determined by tensile testing of subsize specimens machined from the forgings. Appreciable differences in properties between the body and the stem of the B and S forgings are apparent.

Metallographic sections were taken in the same orientation as the specimens for transmission electron microscopy (Figure 7). The orientation of the metallographic and thin foil sections from the body of the forgings was selected to show structure through the wall thickness on a plane parallel to the longitudinal axis of the forging and perpendicular to the inner and outer surfaces of the body wall. This orientation shows the microstructure through which a crack originating on the inner surface of the body cavity would travel, and shows residual effects of forging on microstructure. In one forging, thin foils from three mutually perpendicular orientations were examined by transmission electron microscopy. As discussed later, the substructures in all three orientations were quite similar.

Thin slices for electron microscope examination were cut from the forgings with a diamond saw and reduced to about 0.25-mm (0.010 in.) thick by lap grinding. Discs 3 mm (0.125 in.) in diameter were punched from the thinned slices and electropolished in a CrO_3 acetic acid H_2O electrolyte. The electropolished discs were examined in a Phillips EM 400 transmission electron microscope operated at a voltage of 120 kV. Dislocation densities were determined by techniques described in detail in the literature,[26-28] assuming a foil thickness of 1000 Å.

Results and Discussion

This section describes the microstructures and substructures of the body and stem of each forging described in the Experimental Procedure section. The Conclusion section compares the results of all the forgings (see Table 5) and presents concluding comments regarding the observations.

A. Structure and Properties of A Forging (304L)

Figure 8 shows the microstructure of the body and stem of the A forging. The grain size of the

FIGURE 6. Cross Sectional Drawings and Grain Flow Requirements for the Five Cap Forgings: A and R (304L), and B, L, and S (21-6-9)

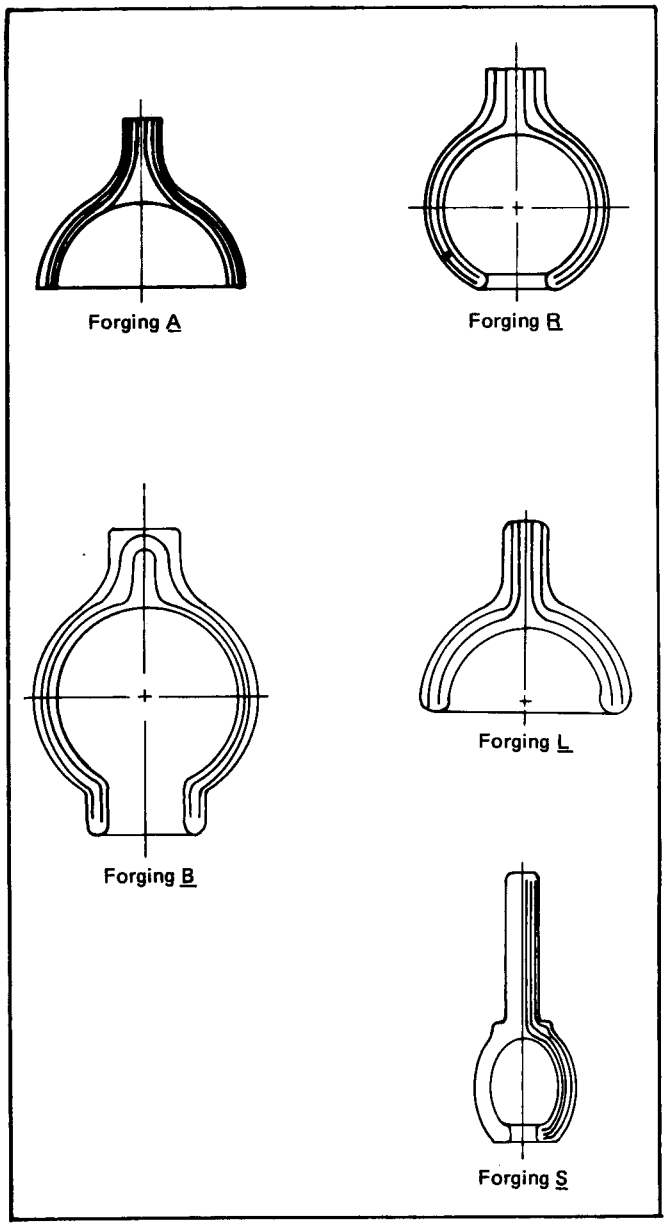

TABLE 3. Processing History of HERF Processed Forgings

	A† (304L)		R† (304L)		B† (21-6-9)		L† (21-6-9)		S† (21-6-9)	
	(°C)	(T/T_m)	(°C)	(T/T_m)	(°C)	(T/T_m)	(°C)	(T/T_m)	(°C)	(T/T_m)
1st Stage*	1040	0.78	1010	0.77	1010	0.79	1040	0.81	1010	0.79
2nd Stage	1010	0.77	980	0.75	980	0.77	980	0.77	840	0.68
3rd Stage	955	0.73	540	0.49	540	0.50	925	0.74	800	0.66
4th Stage	–	–	870	0.68	870	0.70	925	0.74	760	0.63
5th Stage**	–	–	870	0.68	870	0.70	–	–	760	0.63
Final Condition	Annealed***		Annealed***		As Forged		As Forged		As Forged	

*1st Stage - Nominally 2 blows
**Last Stage - Nominally 1 blow
All stages are followed by an immediate water quench.
***Annealing treatment: 1550 °F, 5 minutes at temperature and water quench
†Internal Rocky Flats Designation

TABLE 4. Tensile Properties of HERF Processed Stainless Steel Cap Forgings

Material	Designation†	0.2% Y.S. (ksi)	0.2% Y.S. (MPa)	Ultimate (ksi)	Ultimate (MPa)	Elongation (%)	R.A. (%)	Uniform Elongation (%)
304L	A Body	61.5 (50)*	418 (344)	96.0 (85)	661 (586)	55.8 (35)	88.2 (40)	(25)
	A Stem	50.9	351	89.2	615	65.1	77.3	
304L	R Body	56.3 (50)	388 (344)	94.0 (85)	648 (586)	57.8 (35)	88.8 (40)	(25)
	R Stem	46.3	319	89.2	615	64.6	75.0	
21-6-9	B Body	103.7 (90)	715 (620)	129.1 (120)	889 (830)	36.4 (25)	69.6 (45)	
	B Stem	88.0	606	123.2	849	47.6	69.4	
21-6-9	L Body	82.9 (85)	571 (586)	129.2 (120)	890 (830)	42.4 (30)	69.2 (45)	
	L Stem	80.4	554	123.7	852	46.0	63.4	
21-6-9	S Body	121.2 (116)	835 (800)	136.4 (135)	940 (930)	25.3 (25)	70.2 (45)	
	S Stem	88.6 (65)	610 (450)	125.1 (95)	862 (655)	44.3 (25)	70.9 (45)	

*Values in parentheses were the specified requirements.
†Internal Rocky Flats Designation

stem is slightly larger than that of the body, ASTM 5 versus 6.5, but the body shows more evidence of a deformed structure than the stem. Somewhat elongated grains and curved grain boundaries reflect the more highly deformed body structure. The microstructure is quite clean and free of inclusions. No evidence of grain boundary precipitation is present.

Figures 9 and 10 show the substructure of the body and the stem, respectively, of the A forging. The body shows both well developed subgrains typical of hot work (Figure 9a) and loose dislocation cells typical of a cold worked structure (Figure 9b). The subgrain in Figure 9a is in black contrast relative to the white matrix, an indication of a small orientation difference between the two structures. Figure 10 shows that the substructure of the stem has experienced significantly less deformation than the body after final recrystallization. Dislocations are present at a density of 2 to 5 X 10^{10} cm^{-2} and tend to be uniformly distributed (Figure 10b) in contrast to the high dislocation density arrays in the cell and

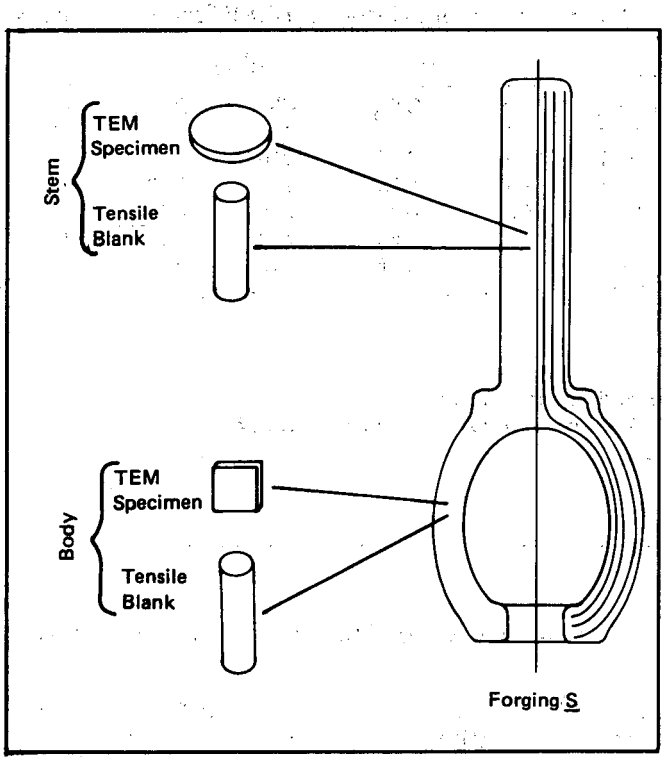

FIGURE 7. Schematic of the Typical Location and Orientation of Tensile Blanks and TEM Specimens in the Bodies and Stems of the Five Cap Forgings

subgrain boundaries of the body. Figure 10a is included to show a network of extended dislocations and an extended node that has formed as a result of dislocation interaction in the low stacking fault energy 304L.[29]

Table 4 shows that the yield strength of the stem of the A forging is about 10 ksi (69 MPa) lower than that of the body, an observation that correlates well with the microstructure and substructure differences noted above. The origin of the differences in properties and structure is, in turn, related to the processing history (Table 3). The stems of the cap forgings are formed first and receive little or no deformation as the body is shaped. If the initial processing stage is performed at a temperature high enough to produce a recrystallized, equiaxed grain structure, as is apparently the case for the forging, the same structure will be retained through the final forming stages. This is consistent with the grain structure (Figure 8b), and the dislocation structure shown in Figure 10. The body, however, is shaped in the last stages, and because of the high strain rate deformation, a cold worked dislocation substructure results even at the relatively high finishing temperature of 0.73 T_m. The A 304L forging has been subjected to a short anneal at 1550 °F (845 °C) but little evidence of recovery as a result of this treatment is visible in the substructure. The as-forged body would be expected to have a yield strength of about 70 ksi (438 MPa)[5] and, therefore, even though not discernible, some stress relief and recovery must have occurred as a result of annealing.

B. Structure and Properties of R Forging (304L)

Figure 11 shows that the grain size of the body is significantly finer than that of the stem (ASTM No. 8.5 versus 5.0, respectively) in the R forging. Again, as the stem was formed first, recrystallization to a relatively coarse grain structure must have occurred in the first, high temperature blows. Likewise, the recrystallization of the

TABLE 5. Summary of Structures of HERF Processed Stainless Steel Forgings

Forging Identification* and Material	Forging Area	Yield Strength	ASTM Grain Size No.	Etch Pitting	Substructure
A (304L)	Body	61.5	6.5	Very Little	Well developed dislocation cells and deformation subgrains
	Stem	50.9	5.0	Very Little	Uniform distribution of dislocations at a density of 2 to 5 X 10^{10} cm^{-2}. No cells or subgrains observed.
R (304L)	Body	56.3	8.5	Very Little	Well developed deformation subgrains; high dislocation density tending to uniform arrays rather than cell structure.
	Stem	46.3	5.0	Very Little	Polygonized subgrains indicating recovery of dislocation structure.
B (21-6-9)	Body	103.7	Variable Across Shear Band	Heavy	Fine recrystallization nuclei near grain boundaries of larger deformed and recovered grains.
	Stem	88.0	8.0	Light	Uniform distribution of dislocations at a density of 1 X 10^{10} cm^{-2}.
L (21-6-9)	Body	82.9	8.5 (Deformed) 12 (Recrystallized)	Heavy	Uniform distribution of dislocations, approximately 20% recrystallization.
	Stem	80.4	10.0	Heavy	Uniform distribution of dislocations with some polygonized subgrains.
S (21-6-9)	Body	121.2	7.5	Heavy	Very uniform dislocation cell structure with cell diameter of 0.22 μm, indicating a highly cold worked structure; also deformation subgrains are present.
	Stem	88.6	9.5	Heavy	Uniform distribution of well separated dislocations in fine, equiaxed grain structure.

*Internal Rocky Flats Designation

FIGURE 8. Microstructure of the A Forging.
(a) Body and (b) Stem; Light Micrographs.

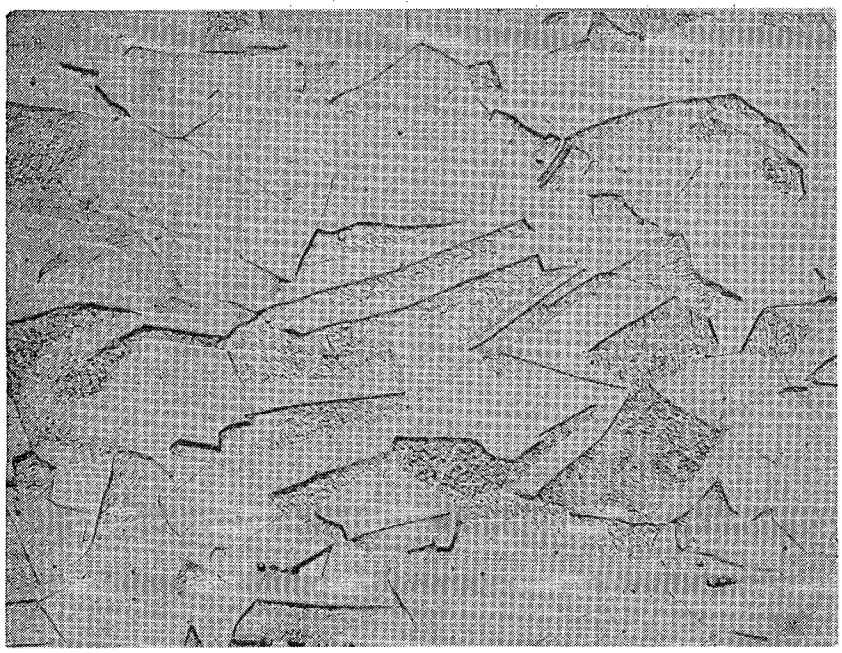

(b) 400X

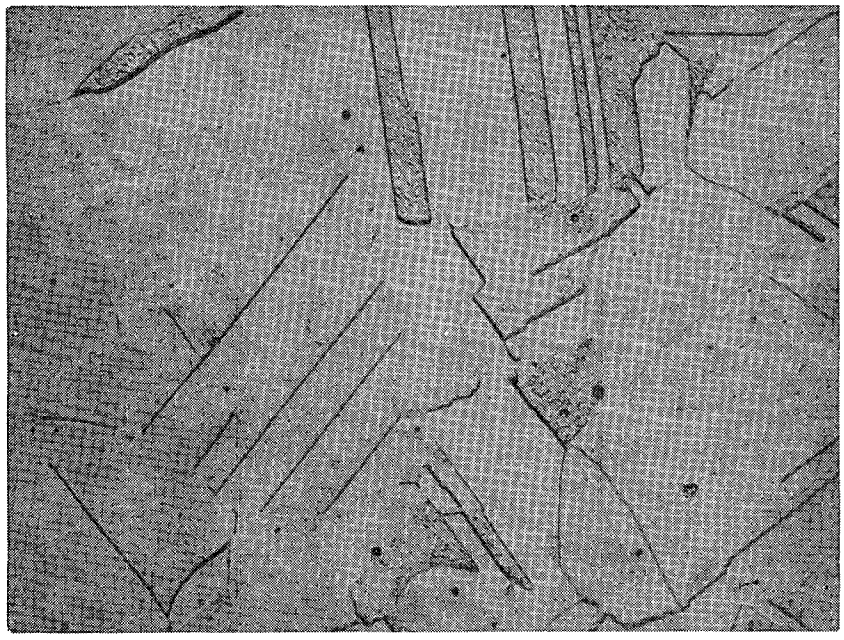

FIGURE 9. Substructure in Body of A Forging. (a) Subgrains, and (b) Dislocation Cell Structure; TEM Micrographs.

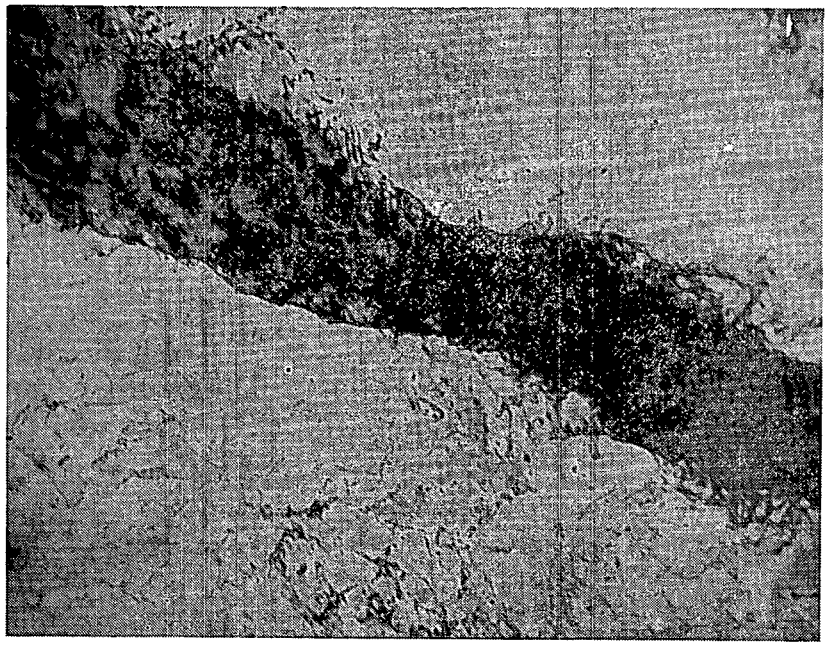

(a) 49,500X

(b) 88,000X

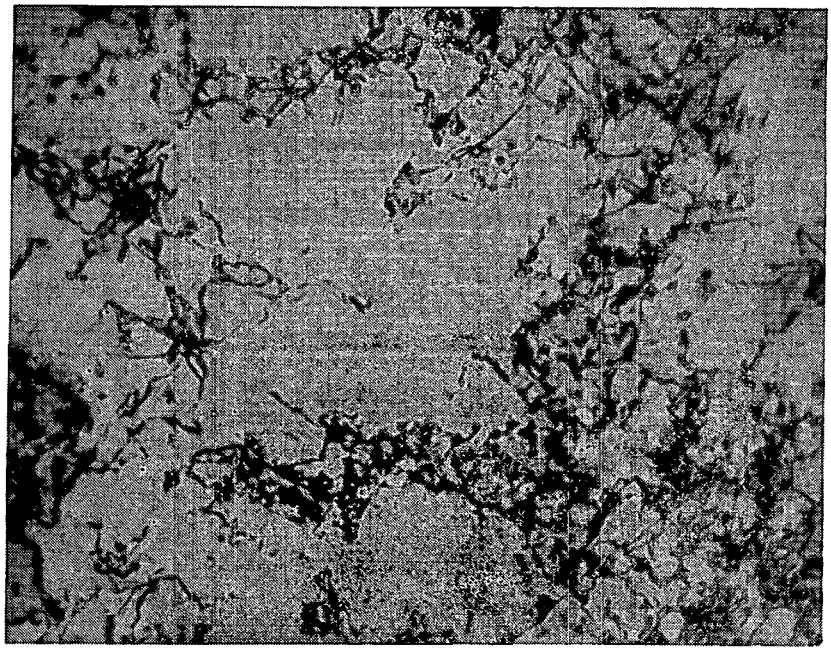

FIGURE 10. Substructure in Stem of A forging. (a) Network of Extended Dislocation Nodes (arrow), and (b) Uniform Distribution of Dislocations; TEM Micrographs.

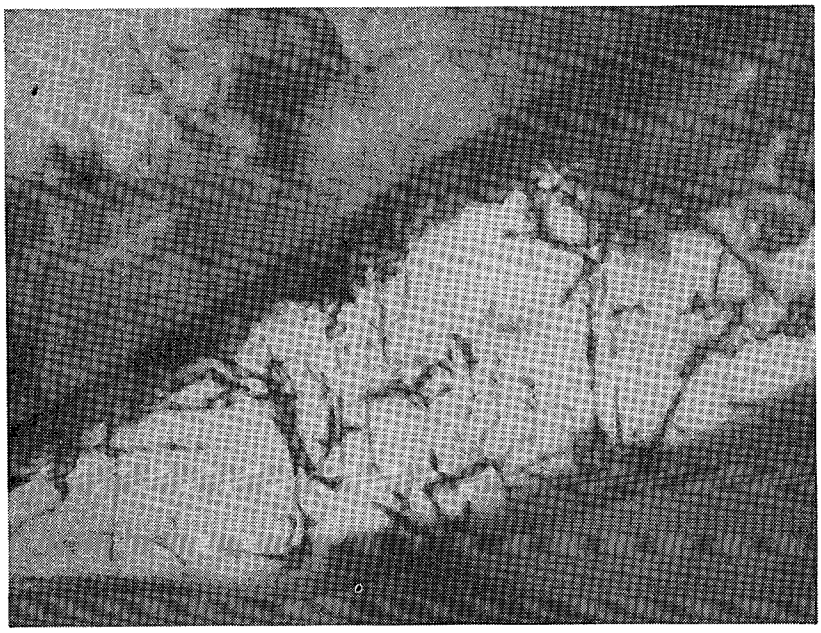

(a) 83,000X

(b) 83,000X

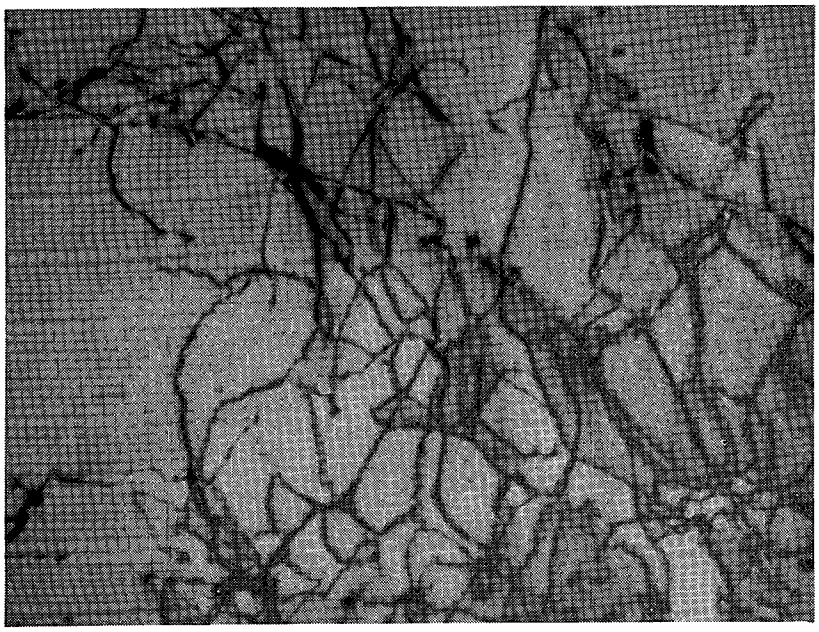

FIGURE 11. Microstructure of R Forging. (a) Body and (b) Stem: Light Micrographs.

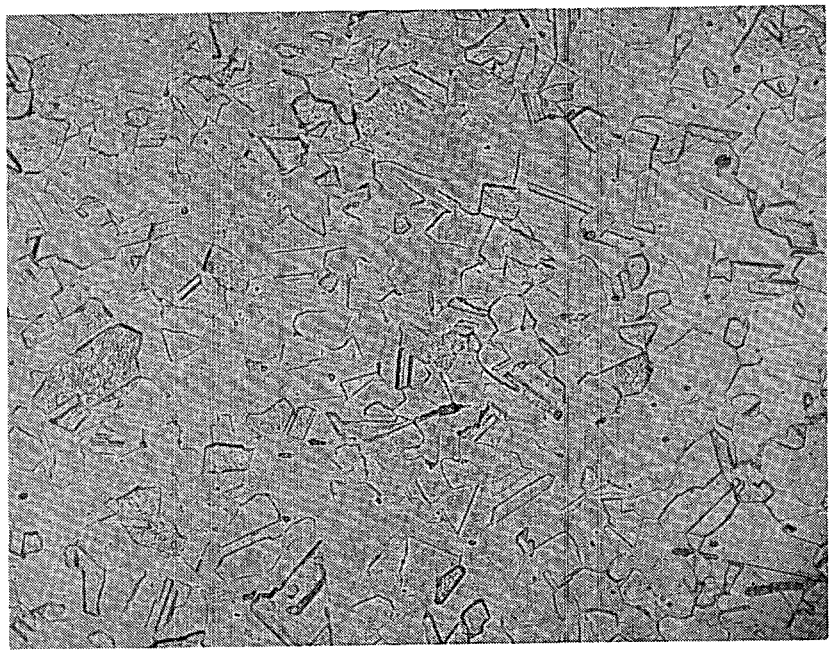

(a) 400X

(b)

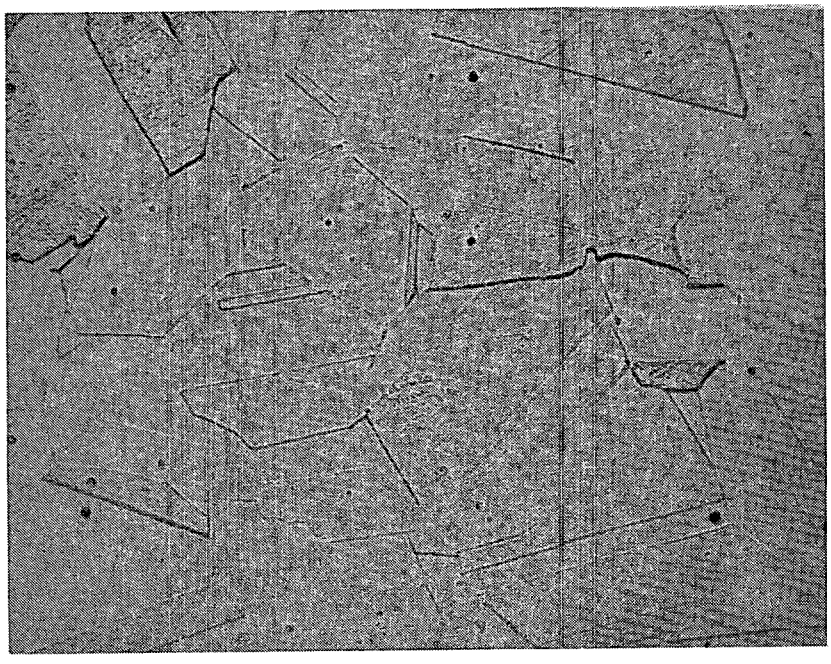

body must have occurred in the early, high temperature deformation stages and because of the more severe deformation of the R forging body, a finer hot worked recrystallized grain size developed. Grain growth during heating for the shaping of the body may also have contributed to the coarse grain size of the stem.

Figure 12 shows that a well defined substructure is present in both the body and stem of the R forging. The body substructure is typical of a deformed structure with well defined subgrains and a high dislocation density (Figure 12a). On the other hand, the substructure of the stem is characteristic of a well recovered, polygonized stainless steel. A well developed low angle dislocation boundary is shown in Figure 12b and provides evidence that dislocations were produced in the stem as the body was shaped. These dislocations have subsequently polygonized during the heating for the body deformation.

The yield strengths of the body and stem of the R forging were 56 ksi (386 MPa) and 46 ksi (317 MPa), respectively, and are consistent with the observed substructures. However, the body yield strength of the R forging was lower than that of the A forging despite the finer grain size of the former. The only difference in structure that explains this strength difference between the two 304L forgings is a slightly less well developed dislocation cell structure in the R forging.

C. Structure and Properties of B Forging (21-6-9)

Figure 13a shows a macrograph through the wall of the B forging and Figures 13b through 13e show the microstructures present at the various locations in Figure 13a. A striking feature of the microstructure of the body is the light etching shear band visible in Figure 13a. Figure 13c shows that this band is composed of highly deformed grains and very fine equiaxed grains with a very high density of etch pits along the grain boundaries. The grain size in the balance of the wall is quite variable and somewhat more equiaxed although there is still considerable evidence for deformation in the form of elongated grains and curved twin and grain boundaries. The density of pits observed appears to be directly proportional to the amount of deformation in the grains except in the shear band. The stem microstructure is much more uniform. The grains are large equiaxed but the twin and grain boundaries do show some curvature, thus indicating some deformation of the worked recrystallized stem microstructure. The pit density is significantly lower in the stem.

Figure 14 shows the substructure of the B forging. The dislocation density of the body is quite high, but small areas on the order of 0.5 μm, with a very low dislocation density, are present throughout the deformed microstructure. Such dislocation-free areas are frequently bounded by regular dislocation arrays and appear to be recrystallization nuclei similar to those reported in the literature.[30] The stem substructure (Figure 14b) consists of dislocations that are widely spaced or arrayed on loose, incipient cell boundaries. Subgrains and well established dislocation cells were not observed.

Selective etching experiments have shown[11] that oxalic acid etching of the body of the 21-6-9 B forging develops a much higher density of pits than does Murakami's reagent. Both oxalic acid and Murakami's reagent are known to reveal carbides, but only the oxalic acid etches grain boundaries and carbides. Therefore, many of the pits revealed by oxalic acid etching in Figure 13 may be due to etching of the boundaries of the fine recrystallization nuclei similar to that shown in Figure 14a. The recrystallization nuclei have no doubt formed because of the very high degree of strain energy and high dislocation density introduced by the forging of the body. The higher the deformation, as in Figure 13c, the more pits; possibly the result of a greater amount of incipient recrystallization. The nuclei apparently formed before cooling after the last processing step. The basis for the latter conclusion is that the nuclei are relatively dislocation free and, therefore, have not been subjected to any significant deformation after their formation. Also, no annealing treatment that might have driven the recrystallization was performed after forging.

The higher yield strength of the body, 104 ksi (717 MPa) compared to that of the stem, 88 ksi (607 MPa), is consistent with the differences in

FIGURE 12. Substructure of R Forging. (a) Deformation subgrains in the Body and (b) Polygonization in Stem; TEM Micrographs.

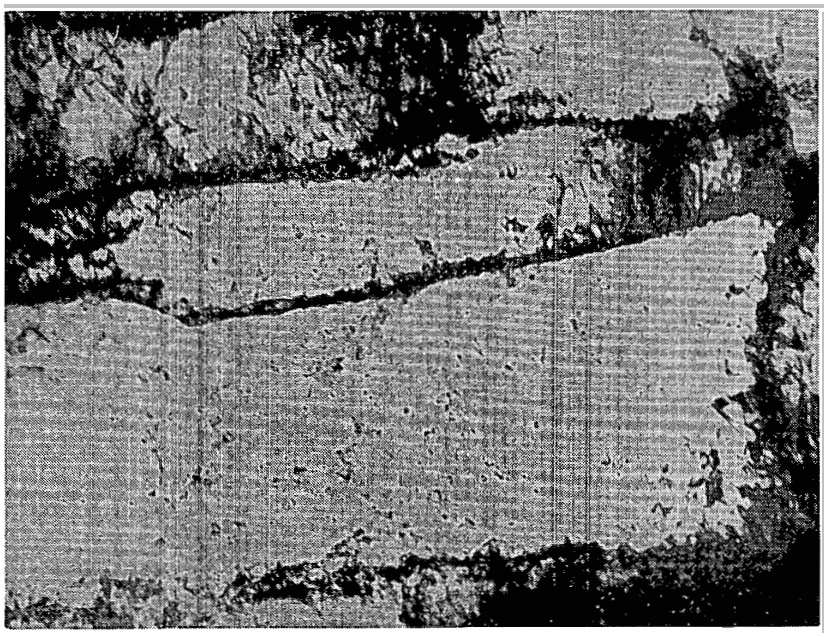

(a) 68,300X

(b) 112,000X

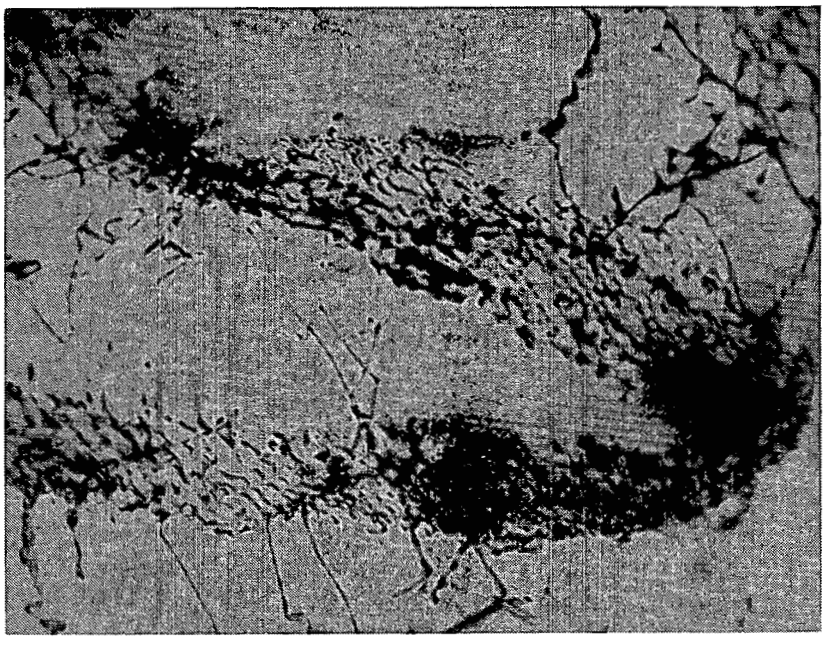

FIGURE 13. Microstructure of the B Forging (21-6-9). (a) Photomacrograph of Body Showing Light Etching Deformation Band and (b) Location 1.

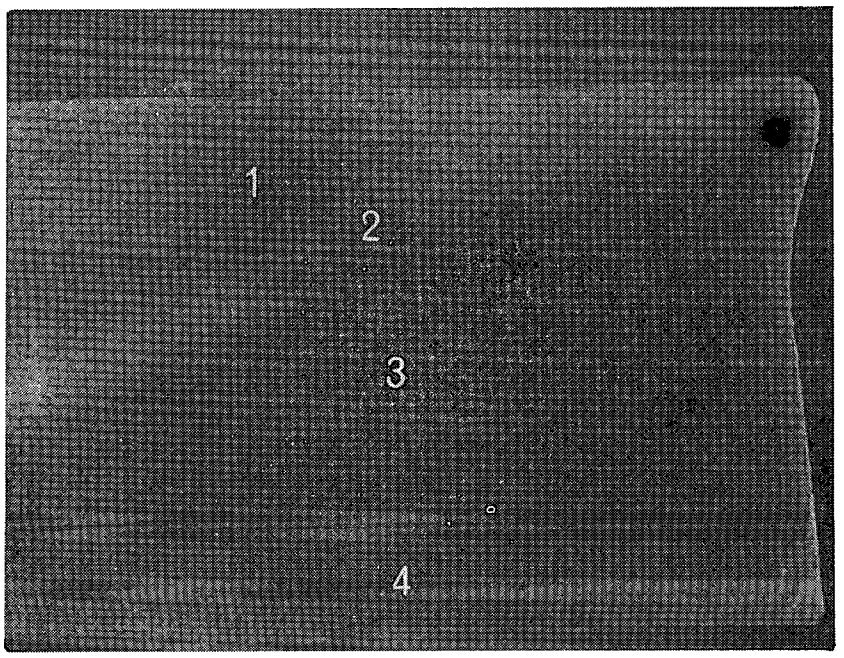

(a) 5X

(b) Location 1 400X

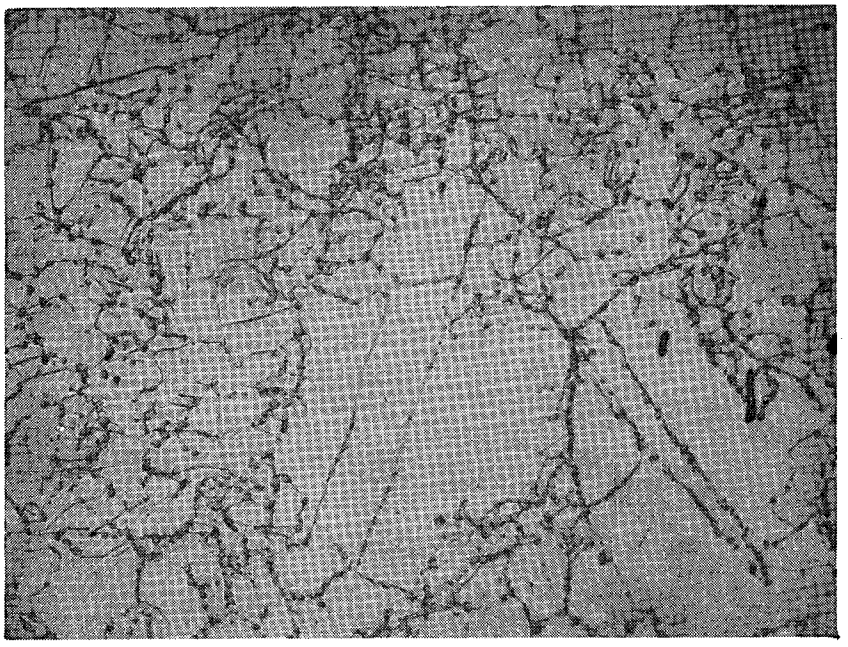

FIGURE 13 (continued). Microstructure of the B Forging (21-6-9). (c) Location 2 and (d) Location 3.

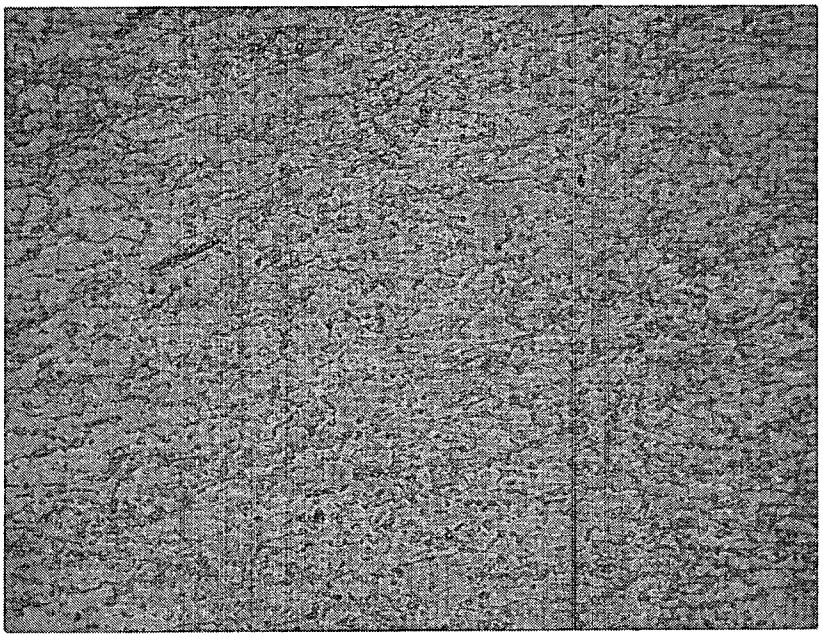

(c) Location 2 400X

(d) Location 3 400X

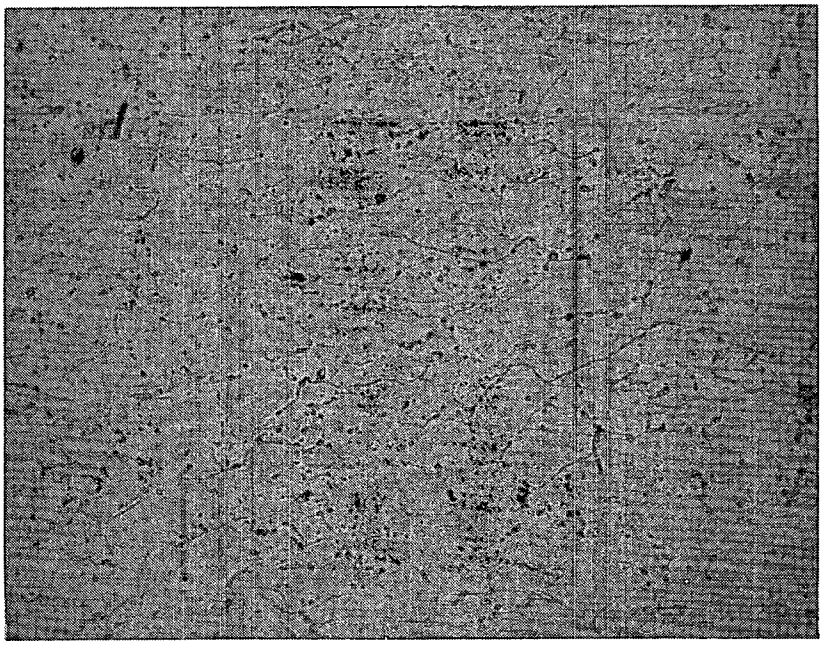

FIGURE 13 (concluded). Microstructure of the B Forging (21-6-9). (e) Location 4 and (f) Stem; Light Micrographs.

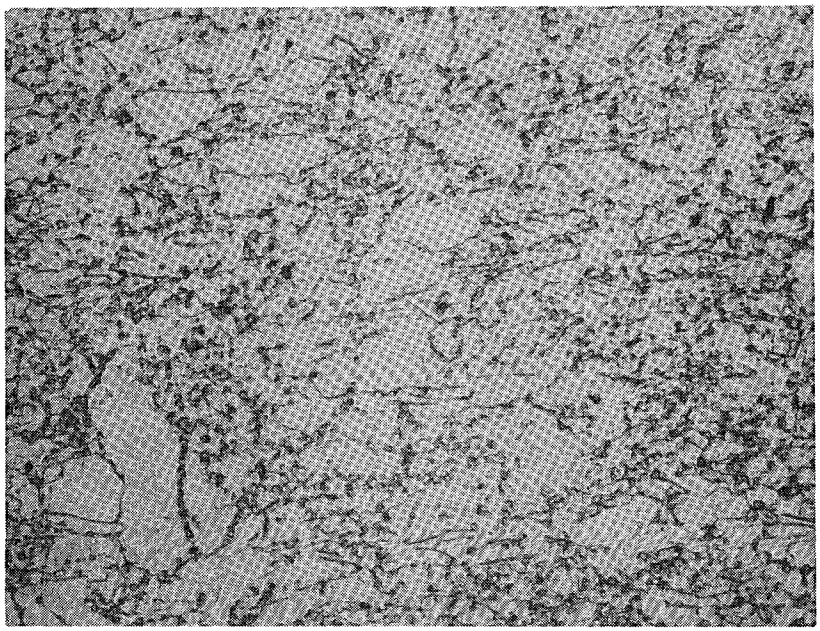

(e) Location 4 400X

(f) Stem 400X

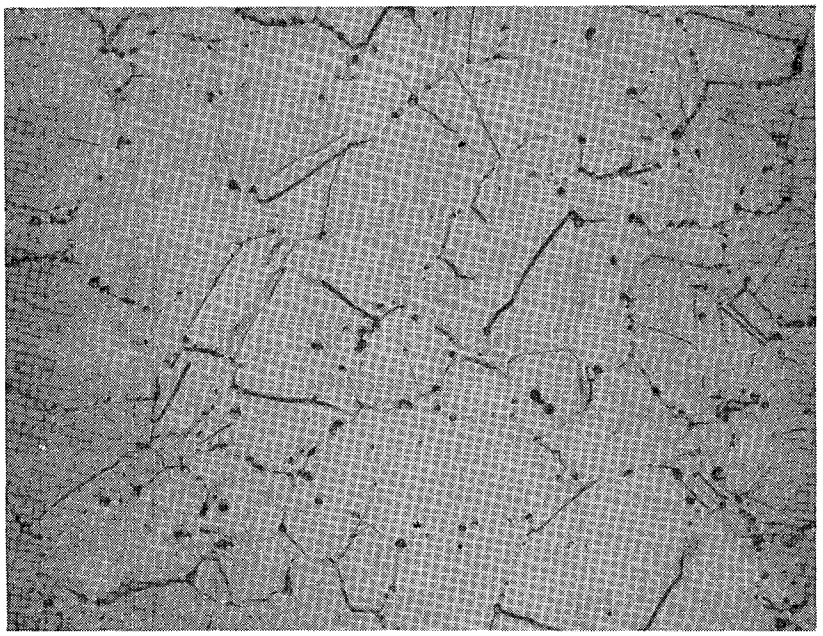

FIGURE 14. Substructure of B Forging. (a) Fine recrystallized grain (A) in Deformed Matrix of Body and (b) Uniform Dislocation Array in Stem; TEM Micrographs.

(a)

(b)

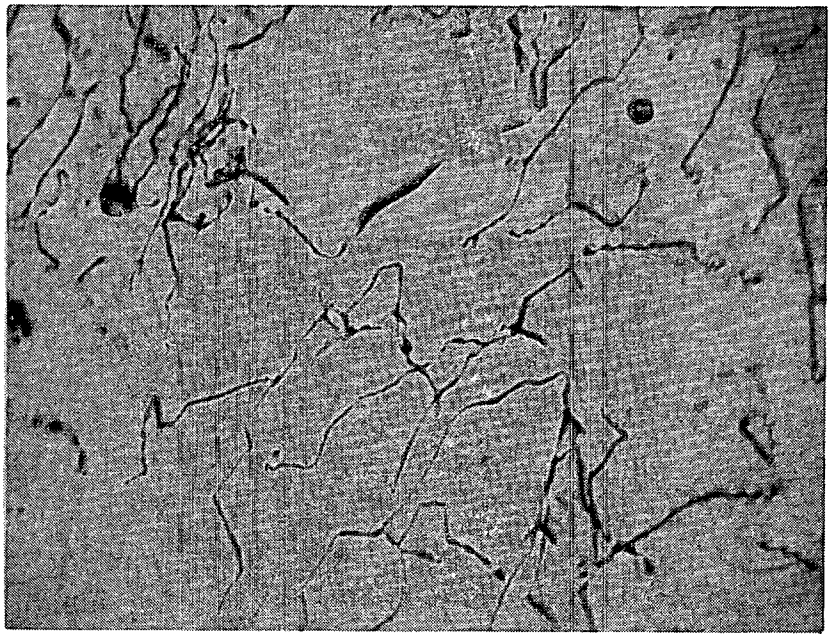

microstructures and substructures of the B forging. Despite the heavy residual deformation, however, the beginning recrystallization and attendant recovery have produced a lower body strength than achievable with a highly cold worked structure without any recrystallization. As discussed in Part E of this report, the body of the S forging which showed no recrystallization and only a highly developed dislocation cell structure had a yield strength of 121 ksi (835 MPa); a yield strength significantly higher than that of the B forging body.

D. Structure and Properties of L Forging (21-6-9)

Figure 15 shows the microstructure of the L forging. The grain size of the stem is finer than that of the body, indicating more deformation of the stem prior to recrystallization in the early high temperature deformation stages. The coarser grain size of the body, however, appears to be more severely deformed but, in fact, has partially recrystallized. Many fine recrystallized grains, intermediate in size between the coarser grains and the fine pits, are present throughout the coarser deformed structure. In contrast, the grain structure of the stem is quite equiaxed. Relatively heavy etch pitting is also present in the body and the stem microstructures.

Figures 16 and 17 show substructures in the body and the stem, respectively. Comparison of Figures 16a and 17a show very similar dislocation structures in the body and stem. The dislocations are loosely tangled, with incipient cell boundaries present in the body and more regular dislocation networks developing in the stem. The latter networks and the polygonized subgrain shown in Figure 17b are evidence for recovery of the stem dislocation structure during later stages of deformation. Figure 16b shows one of several groups of precipitate particles found in thin foils taken from the body of the L forging. These particles were identified as $M_{23}C_6$ carbides. However, the particle density observed in the thin foils did not appear to be as high as the density of pits observed in the light microscope.

The almost identical yield strengths, 83 ksi (573 MPa) and 80 ksi (552 MPa), for the body and the stem, respectively, agreed well with the very similar dislocation structures noted in the two parts of the forging. The low yield strength of the L forging body compared to those of the B and S 21-6-9 is due to the greater degree of recrystallization in the former. (Faintly visible in Figure 15a.) Comparison of the strength of the stem of the L forging with that of the stem of the B forging shows that the L forging has a lower yield strength. This may be explained by the greater degree of recovery noted in the L specimen because of its higher finishing temperature.

E. Structure and Properties of S Forging (21-6-9)

Figure 18a shows that the microstructure of the body of the S forging is deformed; the grains are elongated and evidence for deformation substructure is faintly visible within the grains. The stem grain structure, Figure 18b, is quite fine and equiaxed. Little evidence of deformation is visible.

Figures 19 and 20 show the substructure of the S forging. A very uniform, highly developed dislocation cell structure is visible in Figures 19a and 20a. Also frequently observed in the body were areas of subgrains containing dislocation cells such as shown in Figure 19a. These subgrain areas most probably correspond to the deformation substructures visible in the light micrographs. Thin foils in three mutually perpendicular orientations were taken from the body of forging S and similar cell and subgrain structures were found in all orientations. The dislocation free lengths within the cells were measured on micrographs from specimens in all three orientations, and averaged 0.24, 0.20, and 0.22 μm. The latter result shows that the cells are uniformly developed in the volume of the forging body and are essentially spherical. Somewhat larger cell sizes were measured earlier in HERF processed toroids.[1]

Figure 20b shows the substructure of the stem of the S forging. The grains and twin boundaries are quite straight and show no effects of deformation. The dislocations present are well separated and present in a density of 1×10^{10} cm^{-2}. Comparison of Figures 20a and 20b show the great differences in the substructures of the body and stem of the S forging. The stem must have recrystallized to the very fine equiaxed grain structure shown, and then

FIGURE 15. Microstructure of L Forging.
(a) Body and (b) Stem; Light Micrographs.

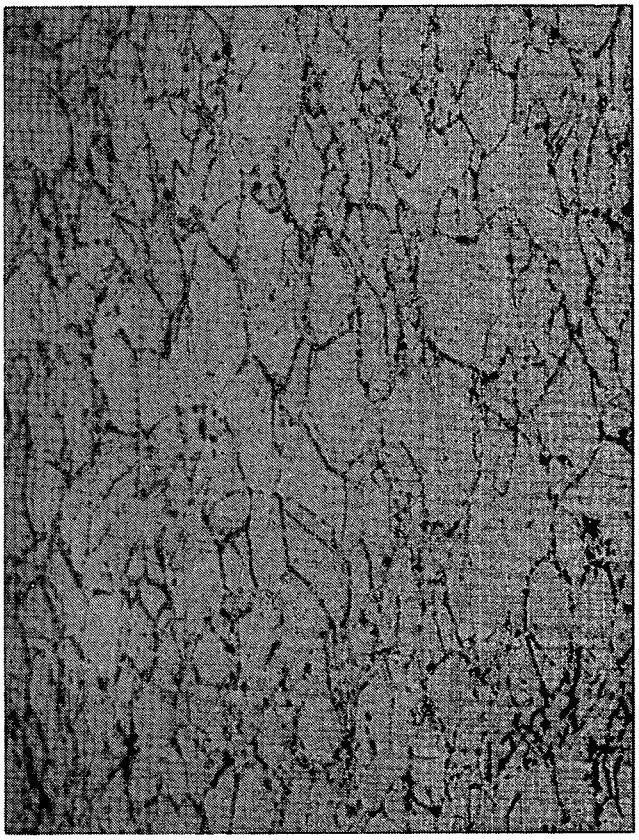

(a) 400X

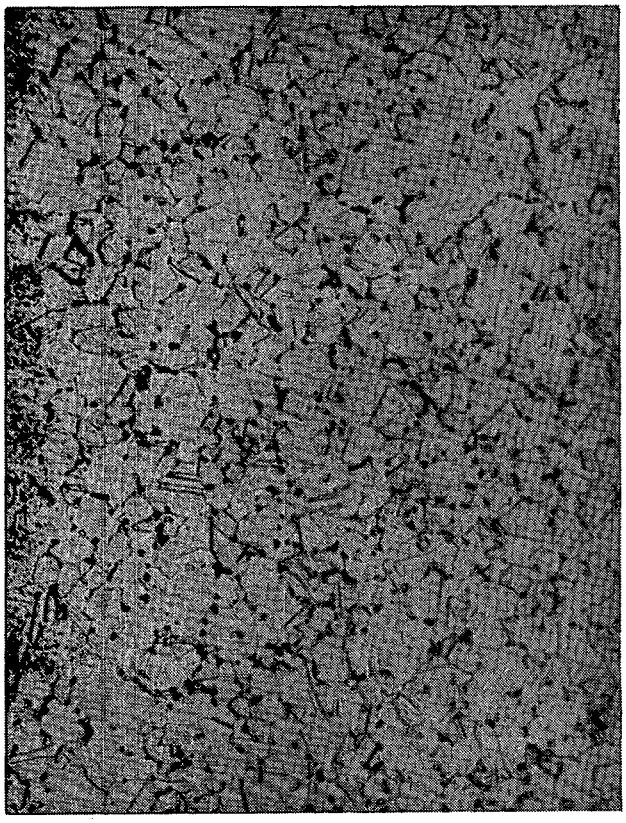

(b) 400X

FIGURE 16. Substructure in Body of L Forging. (a) Dislocations and (b) Grain Boundary Carbides; TEM Micrographs.

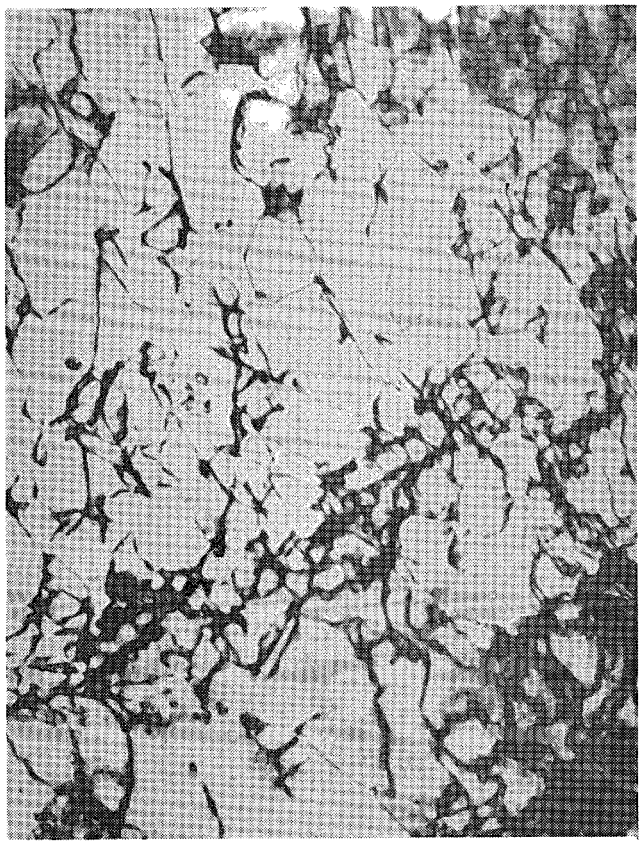

(a) 88,000X

(b) 40,000X

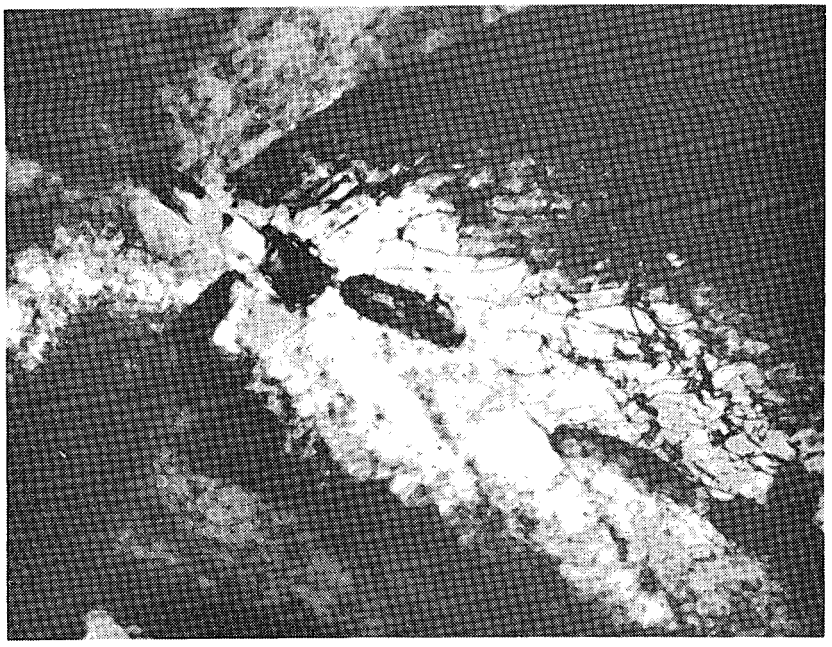

FIGURE 17. Substructure in Stem of L Forging. (a) Dislocation Networks and (b) Subgrain Boundary; TEM Micrographs.

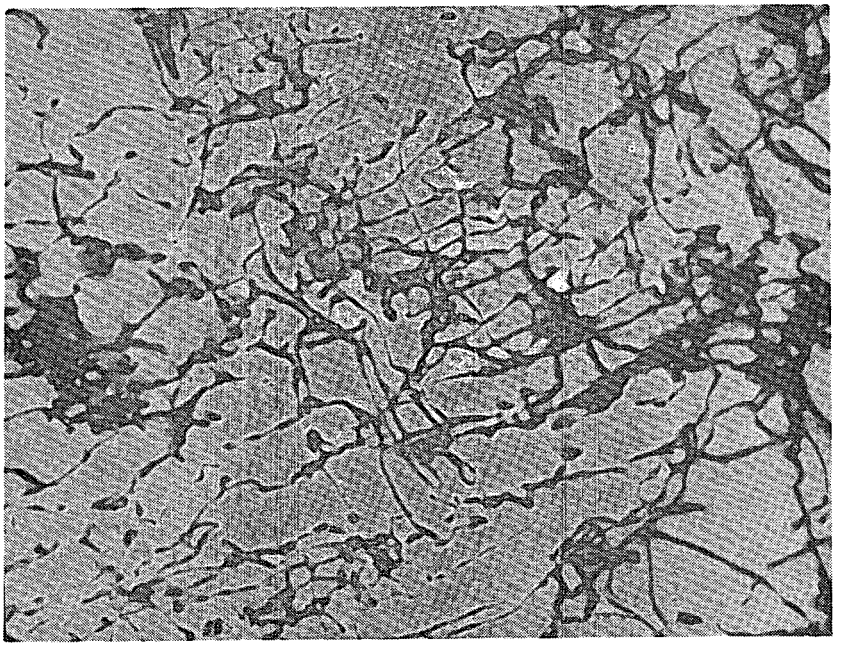

(a) 88,000X

(b) 144,000X

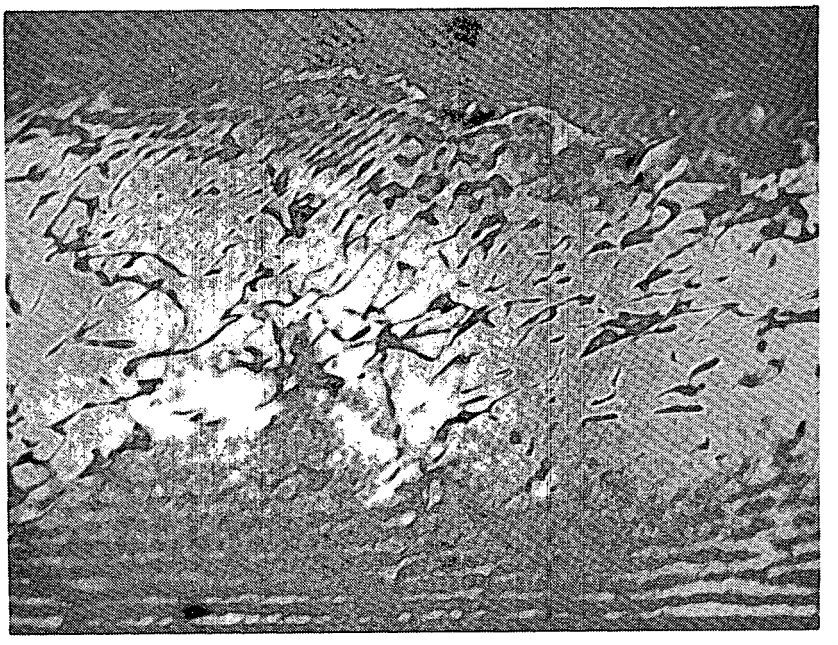

FIGURE 18. Microstructure of S Forging.
(a) Body and (b) Stem; Light Micrographs.

(a) 400X

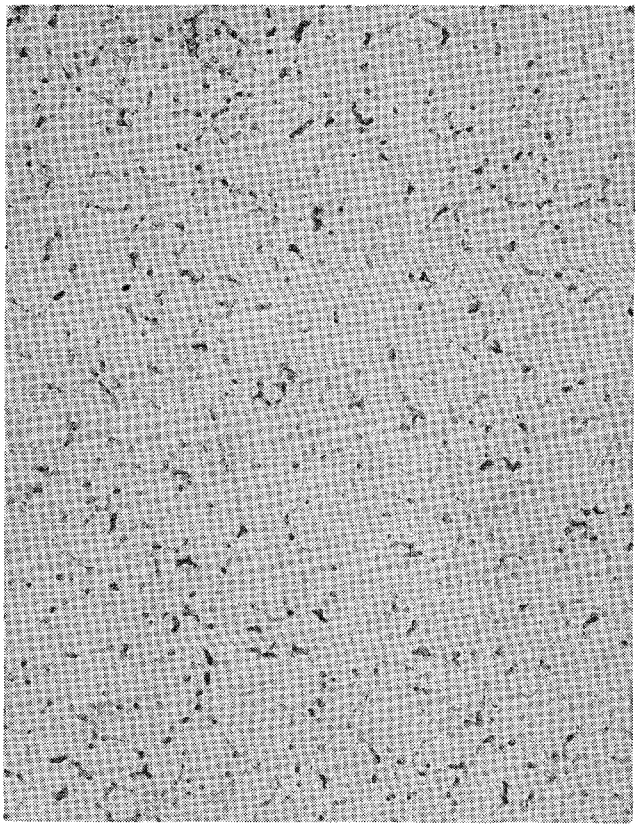

(b) 400X

FIGURE 19. Substructure in Body of S Forging. (a) Dislocation Cell Structure and (b) Deformation Subgrains; TEM Micrographs.

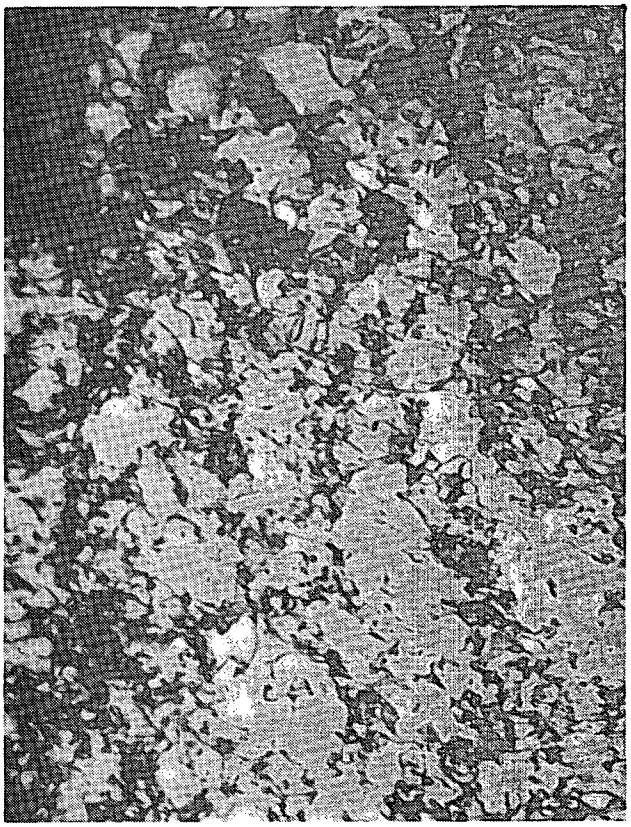

(a) 68,800X

(b) 68,000X

FIGURE 20. Comparison of Subgrains in Body and Stem of S Forging. (a) Dislocation Cells in Body and (b) Fine Recrystallized Grains with Low Dislocation Density in Stem; TEM Micrographs.

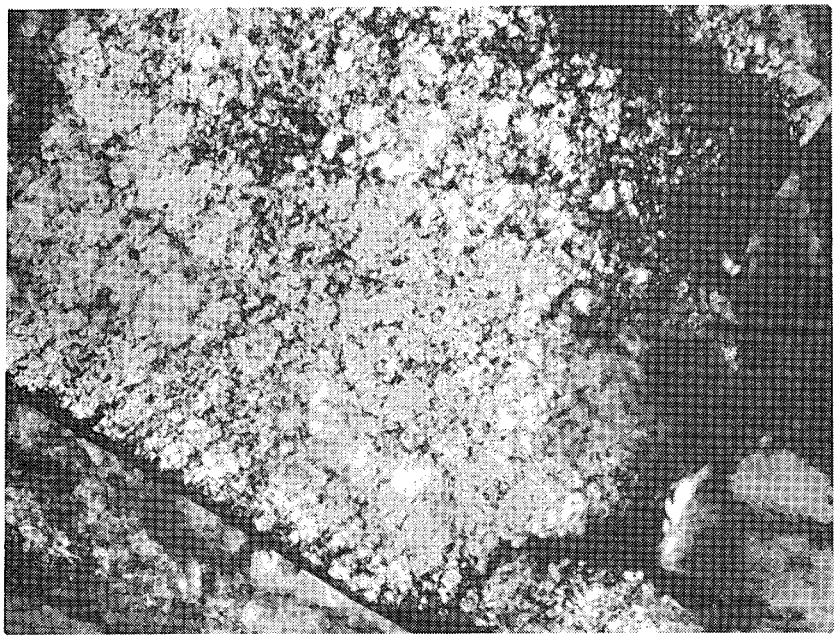

(a) 24,000X

(b) 24,000X

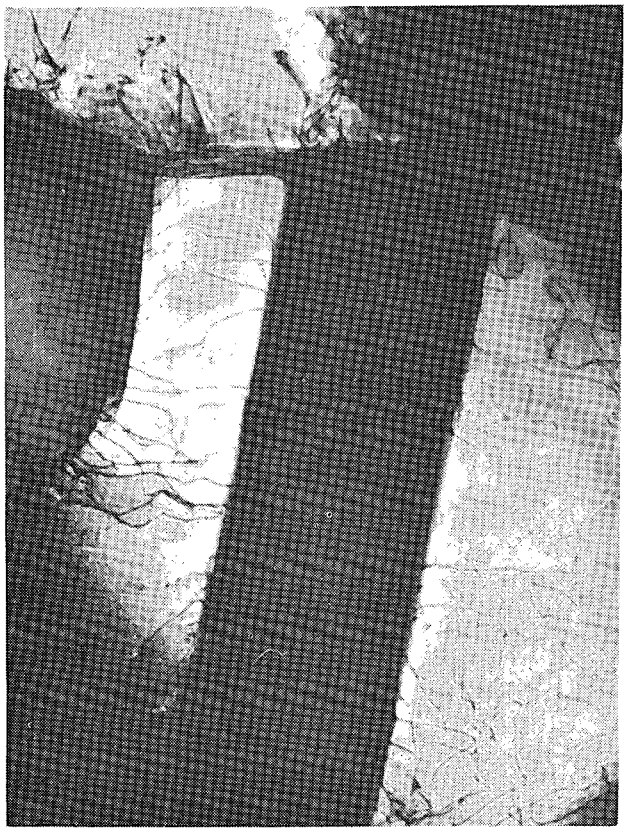

received relatively little deformation as the body was shaped.

There is an excellent correlation between the substructure and mechanical properties of the S forging. The body had the highest yield strength of any of the 21-6-9 forgings (Table 4), in good agreement with the fine, uniform cell structure. The processing schedule for S, Table 3, shows that it was finished at 760 °C, the lowest finishing temperature for any of the 304L and 21-6-9 forgings. The low temperature, high strain rate finishing blows the body have, therefore, produced a highly cold worked dislocation substructure of high strength. The low finishing temperature also seems to have limited recovery of the dislocation structure of the stem, thus maintaining strength at the 88 ksi level.

CONCLUSIONS

Table 5 lists the yield strengths and summarizes the structure characterization of the five HERF processed forgings. A striking general observation regarding this summary is the wide variation in properties and structure not only between the different forgings but also between the stem and the body of the individual forgings. These differences originate in the deformation history of the forgings and the extent of recovery and/or recrystallization that develops during heating of the deformed structure. Some of the correlations among properties, structure, and processing, are summarized below.

The stem of the forging is invariably forged first. The deformation is performed at high temperatures (see Table 3) and the recrystallization that accompanies the hot work produces an equiaxed grain structure in the stem; sometimes as fine as the ASTM 9.5 and 10 measured in the S and L forgings, respectively. Although the stem receives virtually no further deformation as the body is shaped, dislocation densities on the order of 1×10^{10} cm^{-2} are introduced. Generally, these dislocations are well separated and uniformly distributed, and sometimes array themselves into low angle dislocation boundaries, thus producing polygonized subgrains within the equiaxed grain structure. This polygonized type of substructure, most typical of the stems of the 304L R forging and the 21-6-9 L forging, is evidence for recovery that has occurred as the forging was heated for shaping of the body and/or final annealing. The uniform dislocation arrays and polygonized subgrains are responsible for the relatively low strength of the stems.

As noted above, the body of the forgings is shaped last, generally at temperatures low enough to produce a high strength substructure. In fact, the strengths of the bodies of the 21-6-9 forgings appear to be directly related to finishing temperature; the lower the finishing temperature the higher the strength. The basis for this general conclusion, however, is dependent on subtle interactions of deformation and temperature during finishing. For example, the S forging, finished at the lowest temperature, had a highly cold worked substructure characterized by dislocation cells and deformation subgrains. The finishing temperature was apparently low enough to prevent hot working and/or softening by recovery and recrystallization. On the other hand, the B forging, which was finished at an intermediate temperature, apparently was deformed sufficiently and at a high enough temperature to initiate recrystallization during the last deformation stage.

The resolution of the causes of the etch pits observed in the 21-6-9 stainless steel forgings remains an important question. In one instance (the B forging), some of the etch pits have been associated with very fine recrystallization nuclei rather than carbide or inclusion particles. The cause of the high density of etch pits in the other forgings remains unclear, especially in view of the water quenching applied immediately after each blow of the HERF processing.

SUMMARY

Steel forgings discussed in this report are used in applications where specific mechanical properties are required. In most cases, strain hardening is necessary to increase the strength of the 304L and 21-6-9 forgings, so the fabrication process plays a key role in achieving design requirements.

The primary approach in developing required strengths has been to progress through several

iterations of forging sequences until extensive mechanical testing demonstrates that desired properties have been met. Past experience provides some practical guidance in developing multiple blow HERFing procedures. Processes are derived in each case where forging geometry and deformation strain rate are relatively fixed, and forging sequence (i.e., forging temperatures and number of blows at each temperature), are determined from an empirical basis. However, such an approach overlooks the metallurgical behavior of the steel and the benefits that can be gained from an understanding of the substructure that is developed as a result of the various process variables. In addition, the service performance of the finished product is directly dependent upon substructure characteristics in a way that is not completely understood, and which is beyond the scope of the present work. Although substructure examination is only useful as a development tooling and cannot be applied to a routine control of production processing, establishment of relationships between substructure behavior and mechanical properties can provide practical benefits. In this view, greater control of the process would be established and the many instances of anomolous behavior could be better understood. This would also impact the development costs and scheduling delays that typically occur in many instances for problems of unknown origin.

Examples of anomolous behavior have been given in this report. This is indicative that forging processes have not been optimized to the extent desired for adequate control of a production process. Correlating substructure feature with process variables is the only approach left to explain unusual variations in mechanical properties that have been experienced. The observations made in this report introduce the important relationship between substructure and mechanical properties and have put into perspective all the metallurgical considerations that play a role in developing final properties.

Stress relieving introduces another variable into the fabrication process in which the influence on mechanical properties of the forgings cannot be explained in total. It has already been mentioned that high strengths in the forgings are generally maintained, but that variable properties have resulted from the final stress relief. Dead-soft properties have occurred where there is no evidence that the heat treatment was out of control. Such anomolous behavior can only be understood from a microscopic or TEM scale. Evaluating product from optical metallography or tensile properties has been inconclusive. Stress relieving treatments are designed to eliminate residual stresses by causing limited thermal motion of dislocations and thereby stimulating partial recovery of the structure. Theoretically, it is therefore possible to remove residual stresses with only minor dimensional changes and with very little noticeable changes in mechanical properties. The purpose of this work is to establish a basic understanding of the substructure and how it is influenced by various operations within the forging process. The initial work of this study has established such a baseline, and subsequent work can now address such subjects as the effect of stress relief on the substructure of the steel forging.

In addition, significant variations in hardness and corresponding strengths have been experienced both within a single forging and from forging to forging. In this work, it has been shown that there is a distinct transition from dislocation cells to subgrains in the temperature region around 0.5 T_m, depending upon the strain rate of forging. It is not surprising that, with heterogeneous deformation in forgings of complex geometry, the competing processes of recovery and static/dynamic recrystallization can lead to a wide variation in strengths within the structure of the forging. Such variations in properties can occur outside of acceptable limits for design requirements, so metallurgical quality on a substructure scale is important in providing process control.

REFERENCES

1. E. C. Sanderson, A. W. Brewer, R. W. Krenzer, and G. Krauss, Rockwell International, Rocky Flats Plant, RFP-2743, June 24, 1978.

2. H. J. McQueen, *Met. Trans. A.*, Vol. 8A, June 1977, p. 807.

3. A. W. Thompson, *Met. Trans. A.*, Vol. 8A, June 1977, p. 833.

4. Unpublished data, M. C. Mataya, 1978.

5. Private communication with J. Roberts, Rockwell International, Rocky Flats Plant, April 9, 1979.

6. Unpublished data, M. C. Mataya, 1977.

7. Unpublished data, M. C. Mataya, 1976.

8. Unpublished data, M. C. Mataya, 1977.

9. Unpublished data, M. C. Mataya, 1976.

10. C. L. Packard, M. C, Mataya, and C. M. Edstrom, Rockwell International, Rocky Flats Plant, RFP-3031, October 1979.

11. Unpublished data, M. C. Mataya 1979.

12. H. J. McQueen, *J. of Metals,* April 1968, p. 31.

13. W. Roberts and B. Ahlblom, *Acta Met.,* Vol. 26, p. 801.

14. M. J. Lutton and C. M. Sellars, *Acta Met.,* Vol. 17, August 1969, p. 1033.

15. J. J. Jonas, C. M. Sellars, and W. J. McG. Tegart, *Met. Reviews,* No. 130, 1969, p. 1.

16. C. Zener and J. H. Hollomon, *Applied Physics,* Vol. 15, 1944, p. 22.

17. A. M. Sabroff, *Forging Materials and Practices,* Reinhold Book Corp., New York, N. Y., 1968, p. 256–271.

18. C. M. Young and O. D. Sherby, *J. Iron and Steel Institute,* Vol. 211, 1973, p. 640.

19. C. J. Adams and W. M. Williams, *Can. Met. Quarterly,* Vol. 9, 1970, p. 475.

20. Private Communication with P. Armstrong, Lawrence Livermore National Laboratory, August 13, 1979.

21. C.-C. Li, J. D. Flasck, J. A. Yaker, and W. C. Leslie, *Met. Trans. A.,* Vol. 9A, January 1978, p. 85.

22. Unpublished data, M. C. Mataya, 1979.

23. C. L. Packard and C. M. Edstrom, Rockwell International, Rocky Flats Plant, RFP-2897, October 29, 1979.

24. D. J. Michel, J. Moteff, and A. J. Lovell, *Acta Met.,* Vol. 21, September 1973, p. 1269.

25. *Properties and Selection,* Vol. 1, Metals Handbook, Eighth Edition, 1961, p. 422.

26. R. K. Ham, *Phil Mag, 6* (1961), p. 1183.

27. A. S. Keh, *J. Appl. Phys., 31* (1960), p. 1501.

28. C. S. Smith and L. Guttmann, TRANS TMS–AIME, *230,* p. 962, (1964).

29. A. W. Ruff, Jr., *Met. Trans., 1,* p. 2391, (1970).

30. M. Dahlen and L. Winberg, *Acta Metallurgical,* Vol. 28, p. 41, (1980).